ADVANCED MATERIALS
www.advmat.de

Shaping a Soft Future: Patterning Liquid Metals

*Jinwoo Ma, Febby Krisnadi, Man Hou Vong, Minsik Kong, Omar M. Awartani, and Michael D. Dickey**

This review highlights the unique techniques for patterning liquid metals containing gallium (e.g., eutectic gallium indium, EGaIn). These techniques are enabled by two unique attributes of these liquids relative to solid metals: 1) The fluidity of the metal allows it to be injected, sprayed, and generally dispensed. 2) The solid native oxide shell allows the metal to adhere to surfaces and be shaped in ways that would normally be prohibited due to surface tension. The ability to shape liquid metals into non-spherical structures such as wires, antennas, and electrodes can enable fluidic metallic conductors for stretchable electronics, soft robotics, e-skins, and wearables. The key properties of these metals with a focus on methods to pattern liquid metals into soft or stretchable devices are summari.

1. Introduction

This review highlights techniques to control the shape of liquid metals, in particular, low-melting-point gallium-based metals and alloys (such as eutectic gallium indium, EGaIn). Why liquid metals? Liquid metals possess both the properties of metals and liquids. The combination of fluidity and metallic conductivity makes liquid metals uniquely suited for stretchable electronics (e.g., wearable electronics, soft robotics, soft energy harvesters), a growing field that has attracted immense research and commercial interest.

The ability to shape and pattern conductors has always been integral to the fabrication of functional devices. For example, copper ingots can be drawn to form wires, copper films can be patterned lithographically as circuit interconnects, and coiling copper wire into a helix produces an inductor. In short, the shape of the conductor determines its electrical behavior and utility. The same is true for liquid metals. Advances in techniques for shaping liquid metals down to submicrometer scale resolution have enabled a wide range of novel devices, from wearable sensors, to reconfigurable circuits and liquid electronic switches. This is a great motivator for studying the principles of liquid metal patterning and continued research into improving the achievable breadth, scale, and design complexity. Since liquid metals are a subset of liquids, the basic principles described here can extend broadly to other liquids. That being said, owing to certain distinguishing characteristics of liquid metals, not all patterning techniques that work well with other liquids necessarily work well with liquid metals. For example, liquid metals have enormous interfacial tension, which makes it difficult to coerce them into non-spherical, high surface area shapes. Thus, while it may be easy to deposit a thin film of polymer by spin coating, it is not so straightforward to make a thin film of liquid metal. In this review, we start with a general discussion of liquids, and in the subsequent section, we elaborate on the unique features of liquid metals that make them so interesting yet sometimes challenging to manipulate.

It is difficult to manipulate the shape of liquids because of their ability to flow in response to stress into shapes that minimize energy. At larger length scales, gravity typically is the dominant force, while at small length scales, interfacial forces dominate. The capillary length defines the length scale below which interfacial forces become relevant relative to gravitational forces. For most fluids (including liquid metals), this occurs when at least one dimension of the fluid is below ≈1 mm. Interfacial forces conspire to minimize surface energy, thereby making it difficult to create liquids with arbitrary shapes. For example, cylindrical streams of water from a hose or nozzle break into droplets via so-called "Rayleigh-Plateau" instabilities.[1,2] Other forces, such as shear, magnetic fields, and electric fields can distort or manipulate the shape of liquids, but these forces are externally applied and not inherent to the fluid.

Considering these challenges, perhaps the easiest way to manipulate the shape of a liquid is to confine it in a container, as shown in **Figure 1**a. Examples include blood in capillaries or fluids in microfluidic channels. This approach is appealing because it enables fluids with nearly arbitrary shapes.

It is more challenging to pattern liquids without the use of containers. Considering that interfacial forces dominate below

J. Ma, F. Krisnadi, M. H. Vong, M. Kong, M. D. Dickey
Department of Chemical and Biomolecular Engineering
North Carolina State University
Raleigh, NC 27695, USA
E-mail: mddickey@ncsu.edu
O. M. Awartani
Department of Mechanical Engineering
Maroun Semaan Faculty of Engineering and Architecture
American University of Beirut
Beirut 1107-2020, Lebanon
The ORCID identification number(s) for the author(s) of this article can be found under https://doi.org/10.1002/adma.202205196.

DOI: 10.1002/adma.202205196

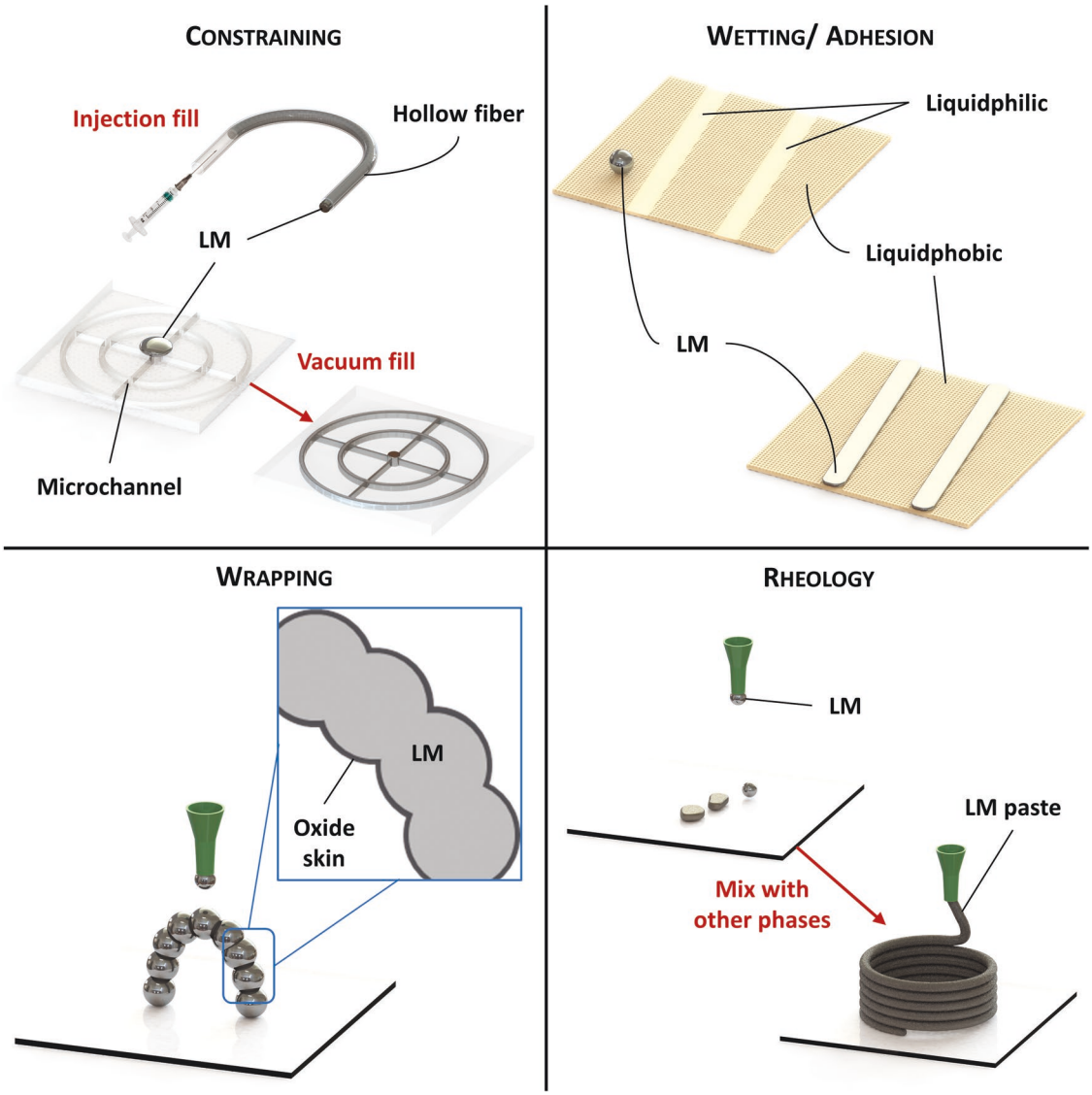

Figure 1. In general, liquids flow to minimize energy, making it difficult to control their shape. There are four general strategies to control the shape of liquids, including liquid metal (LM): a) controlling shape by confining a liquid in a container; b) At small length scales, interfacial energy can be harnessed to coerce liquids to selectively wet surface patterns; c) Wrapping the liquid in a thin film, such as the native oxide skin that forms on LM, can create a mechanical shell that stabilizes unique shapes; d) Adding rheological modifiers to the liquid can limit its ability to flow in response to interfacial force.

the capillary length, such interfacial forces can be utilized to manipulate liquids to selectively wet or adhere to portions of a surface, as conceptualized in Figure 1b. The cross-sectional shape of such patterns is hemispherical, but the in-plane shape can be controlled based on the interactions with the substrate.

If the surface that the liquid wets is sufficiently thin (e.g., a thin film or layer of particles), then the interfacial forces can cause solid-like film to encase the liquid (Figure 1c).[3–5] The resulting structure should still adopt a shape to minimize energy, but in such a case the energetic analysis must account for the mechanical contributions of the "skin". If the liquid (or material in the liquid) is reactive, it is even possible for the skin to spontaneously form around the liquid.[6] For example, gallium liquid metal can react with air to form a native oxide skin (Figure 1c). This approach is fascinating because it allows liquids to form their own container, which is a major theme of this review.

Finally, another route to manipulate liquids into useful shapes is to change the rheological behavior. Liquids with low viscosity, such as water, can flow readily to minimize surface energy. But if the rheological properties are modified, then this behavior can be retarded or even arrested (Figure 1d). This can be done by introducing other immiscible fluids to the liquid to produce a colloidal system that is structured by inclusion-matrix interfaces.[7] The addition of solid inclusions would result in multiphasic mixtures with more elastic character. For example, tooth paste—a mixture of powdered solids and liquids—can be extruded onto a toothbrush and hold its shape. Yet, tooth paste is difficult to extrude through small capillaries, such as a drinking straw. Thus, this approach is not without tradeoffs.

In this review, we focus on patterning and shaping of liquid metals. The approaches utilize the four general approaches for patterning liquids shown in Figure 1. Unlike conventional liquids, such as water, liquid metals offer some truly unique opportunities due to their metallic conductivity (electrical, optical, and thermal) and their ability to rapidly react with oxygen to form a "skin" (similar to Figure 1c). And unlike solid metals, the fluid nature of liquid metals allows them to be manipulated, dispensed, and patterned in ways that simply are not possible with solid metals. These properties allow liquid metals to be used as soft and stretchable electrodes, interconnects, sensors, and microfluidic components. Applications include stretchable electronics, reconfigurable antennas, soft robots, wearable sensors, and e-skins.

We start by comparing liquid metal to water to underscore the distinct attributes of liquid metal. The main body of this review focuses on methods to shape (and reconfigure the shape) of liquid metal due to the importance of controlling the shape and location of materials for most devices. We conclude with an outlook, challenges, and opportunities.

2. Properties and Behavior of Ga-Based Liquid Metals

2.1. What are Liquid Metals?

In the literature, the terms "liquid metal" (LM), "fusible alloy", "liquid metal alloy" (LMA), "low-melting-point alloy" (LMPA) have been used to refer to metals and metal alloys with low enough melting points that they exist as liquids at (or near) room temperature and pressure.[8–11] Here, we use the term "liquid metal" (LM). While the LMs in this review have near-room temperature melting points (up to ≈30 °C), in some other reviews, metals and alloys with melting points up to ≈300 °C are also considered to be LM.[8,12]

There are only five known elemental LMs, namely gallium (melting point, T_m = 29.76 °C), mercury (T_m = −38.83 °C), francium (T_m = 27 °C), cesium (T_m = 28.44 °C), and rubidium (T_m = 39.3 °C). Unfortunately, most of them are not safe for practical use. Cesium and rubidium react violently with gases in the atmosphere,[13] while mercury and francium are toxic and radioactive, respectively.[14,15] Process of elimination leaves gallium, which happens to have some of the most interesting properties of any element: 1) It has low toxicity and effectively zero vapor pressure at room temperature.[16] The latter means it can be handled without concern for breathing it via evaporation. 2) It expands when it freezes, yet it is difficult to freeze since it supercools well below its melting point of 29.76 °C.[17,18] 3) It boils at 2400 °C.[19] 4) It has water-like viscosity (≈2× that of water).[20,21] 5) It is dense (≈6× that of water).[21] 6) It has the largest surface tension of any liquid at room temperature (720 mN m^{-1}, ≈10× that of water).[9,22]

Although gallium's melting point is slightly higher than room temperature,[9,23] it can be mixed with certain metals at certain compositions to produce alloys with even lower melting temperatures than that of their constituents. For example, eutectic gallium indium (EGaIn, 75 wt% Ga and 25 wt% In, T_m = 15.7 °C) and gallium indium tin (Galinstan, 66.5 wt% Ga, 20.5 wt% In, and 13 wt% Sn, T_m = 11 °C) are two alloys with lower than room temperature melting points.[9,23] Henceforth, unless otherwise specified, we imply Ga-based liquid metals when we use the term "LM".

2.2. Passivating Oxide Skin on LMs

Gallium is a post-transition metal that belongs to the 13th column in the periodic table. It resides directly below aluminum. Thus, it is not surprising that gallium forms a passivating oxide very quickly at ambient condition, similar to aluminum.

Although native oxides are thin (typically a few nanometers),[9] their importance for our society cannot be overstated because of their role in protecting metals—such as aluminum and stainless steel—against destructive oxidation. Metals like Al and Ga are extremely reactive and would readily oxidize if it were not for the protective nature of the passivating native oxide layer.

The native oxide forms rapidly at low temperature and even under oxygen deficient environments.[24–27] The growth of native oxides is often described by Cabrera–Mott modeling, which claims that electrons from the metal can tunnel through the surface oxide to combine with oxygen from the air to form an oxy-anion. This results in an electric field between the positively charged metal surface and negatively charged anions that reside across the thin oxide. This field drives these charged species towards each other and causes the oxide to grow. As the oxide thickens, this driving field decreases until the thickness reaches a stable "passivated" value.[28,29] Ligands on the surface can affect the final thickness of the oxide.[30,31]

In the case of LM, the oxidation significantly slows when the thickness reaches ≈3 nm as measured by transmission electron microscopy.[29,31–33] Ga^{3+} is the most stable form of oxidized gallium and the native oxide is thought to be amorphous or poorly crystalline Ga_2O_3 (or slightly off-stoichiometry) based on X-ray grazing-incidence measurements.[34] Despite the incorporation of other secondary metals (such as indium) to lower the melting point of gallium alloys, the surface remains primarily gallium oxide since it is thermodynamically favorable.[35,36] Given that rationale, it is indeed possible to change the composition of the oxide by dissolving metals into LMs that have lower Gibbs free energy of oxidation compared to gallium.[36] For example, it is possible to form aluminum oxide on the surface by adding small amounts of Al to Ga, yet doing so under ambient conditions can result in a breakdown in passivation.[20,36,37] The chemical composition of the gallium oxide could also be tuned by changing the surrounding environment.[31] For example, it converts to GaOOH in water.[38]

2.3. Unique Features of LMs

In this section, we contrast the behavioral differences between water and LMs to highlight unique attributes of LMs, many of which are important for patterning.

2.3.1. The Importance of the Oxide

Due to surface tension, water spontaneously forms hemispherical shapes on substrates to minimize its energy (**Figure 2**a).

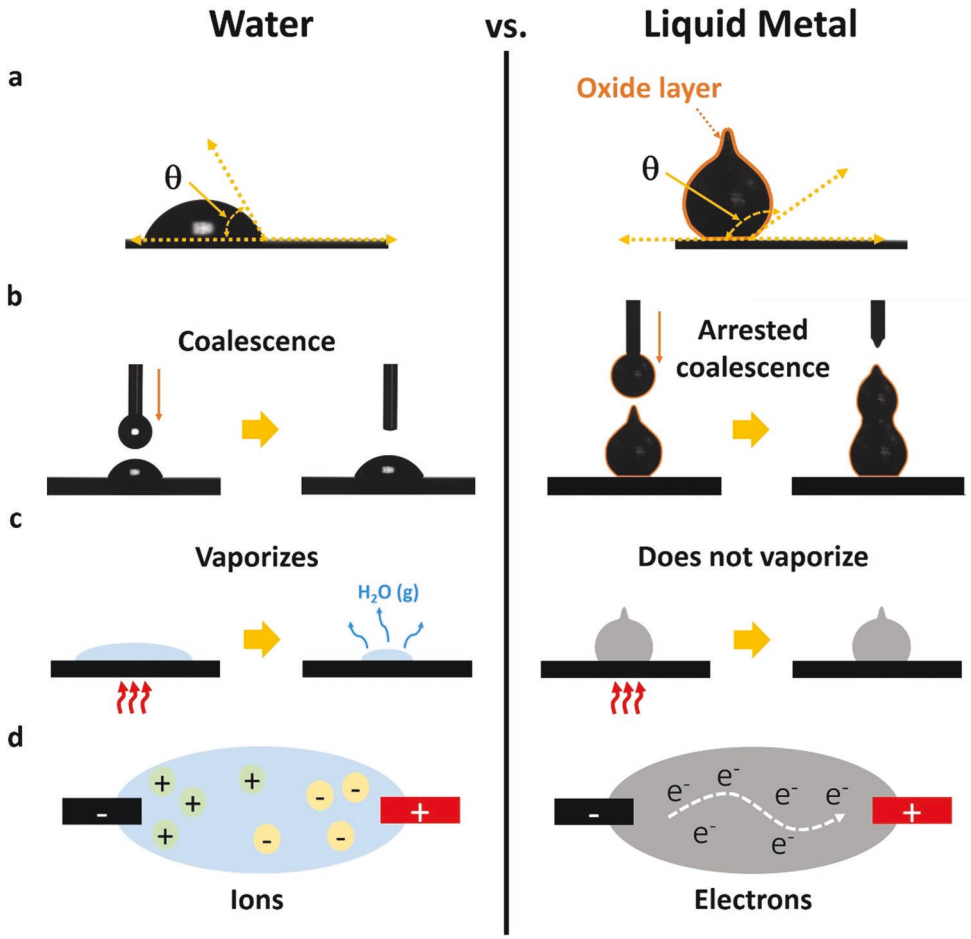

Figure 2. Comparison of water and liquid metal (LM). a) The surface tension of water causes it to adopt a hemispherical shape and form a contact angle θ with a substrate. Although LM has an enormous surface tension, the presence of the oxide can preserve non-spherical shapes (such as the tip on top of the droplet) and prevent the liquid from flowing, complicating contact angle analysis. b) At small length scales, two LM droplets can be stacked vertically without complete coalescence. Conversely, when two water droplets touch, they coalesce. c) Water slowly evaporates and diminishes in volume at room temperature. However, LM has negligible vapor pressure at room temperature. d) Water is an ionic conductor, whereas LM is a metallic conductor.

Although bare metals have enormous surface tension (≈10× that of water) and should therefore form spherical caps like water, the mechanical properties of the oxide stabilize non-spherical shapes, such as cones (Figure 2a).[39] This property is enabling for many methods for patterning LM discussed herein.

Furthermore, the oxide complicates contact angle measurements because the interface of the droplet is not free to flow.[40] Bare LMs, which are free to flow, interact with surfaces primarily by metallic bonding (so-called "reactive wetting") and therefore typically have large θ on non-metallic surfaces. Interestingly, dispensing LM (with the native oxide) on a surface also results in a large apparent contact angle, yet such large angles do not necessarily mean that the substrate is "metallophobic". Instead, the oxide typically causes the droplets to adhere to surfaces since the oxide can form van der Waals or hydrogen bonding interactions with the surface.[41,42] Rough surfaces can minimize adhesion due to the poor contact between the substrate and oxide.[43–45] Due to the mechanical effects of the oxide, advancing and receding contact angles should be utilized rather than static contact angles; the advancing angle is large on all surfaces regardless of surface chemistry due to the need to rupture the oxide, whereas receding provides a measure of whether the oxide adheres (pins) to the substrate.[40]

The surface yield stress of the oxide has been measured via rheological techniques to be ≈0.3–0.5 N m^{-1}.[20,46,47] Because the oxide is a thin surface film that can reform rapidly when it breaks, this value can effectively be considered like an interfacial tension that resists flow. But unlike interfacial tension, the solid oxide film does not drive flow. Although oxides are naturally brittle and break at low strains, the ability of the oxide to rapidly reform on exposed metal means the liquid will stop flowing immediately when the applied stress no longer exceeds the critical value. This unique feature of LM makes it possible to stabilize LM into useful shapes such as wires, strips, and even freestanding 3D structures.[48–50]

When two droplets of water are brought into contact, they coalesce into a larger droplet with a spherical interface (Figure 2b). LMs typically have low bulk viscosity (≈2 cps), comparable to that of water (≈1 cps) and pose little resistance to flow. Yet, LM droplets with diameters of hundreds of micrometers

can be stacked on top of each other without complete coalescence. Upon contact, the oxide breaks and allows the metal in the droplets to make metal–metal contact, but the oxide shell prevents complete coalescence. As the diameter of the droplet gets smaller, it becomes more difficult to merge the droplets. The pressure required scales inversely with diameter.[51] The stability imparted by the oxide makes it easier to incorporate LM particles into polymers and fluid media to form multiphase composites and mixtures.[52–57] Such droplets can be forced to merge into conductive traces, which is a patterning method discussed herein.

In summary, the presence of the oxide skin: 1) changes the mechanical properties of the interface of LM from a liquid to a solid, 2) changes the chemical properties of the interface of LM from a metal to an oxide, 3) replaces the metal/ambient interface with two new interfaces (metal/oxide interface and oxide/ambient interface), thereby separating the metal from the ambient, 4) stabilizes the shape of the metal below a surface stress of ≈0.5 N m^{-1}, and 5) enables adhesion to smooth surfaces.

2.3.2. Volatility

Typical liquids like water and oil evaporate slowly at room temperature, and rapidly approaching their boiling temperatures (100 °C for water, and 200–300 °C for most oils). LMs, on the other hand, have effectively zero vapor pressure at room temperature (Figure 2c). This means that there is no risk of inhaling metal vapors while handling LMs. LMs have extremely high boiling temperatures (e.g., 2400 °C for Ga)[9,58] which makes them suitable for processing and handling outside the fume hood. LMs also do not evaporate at ambient temperatures when placed within a low-pressure environment, such as a vacuum chamber, making them suitable for a variety of spectroscopic studies that require vacuum.

2.3.3. Conductivity

LMs conduct electrons whereas water conducts ions. Consequently, the electrical conductivities of LMs, such as EGaIn,[59] are much higher (6–10 orders of magnitude) than typical liquids like water or even salt water (Figure 2d). For example, the electrical conductivities of EGaIn, Galinstan, and mercury are 3.4×10^6, 3.46×10^6, and 1.0×10^6 S m^{-1}, respectively.[60] On the other hand, the electrical conductivity of water is significantly lower and depends on the concentration of ions (e.g., drinking water and sea water are 5×10^{-4} to 5×10^{-2} and 4.8 S m^{-1}, respectively). LMs also have superior thermal conductivity, >10 W m^{-1} K^{-1} versus ≈0.6 W m^{-1} K^{-1} for water.[61] LMs have constant conductivity even as they flow under applied shear. This is not the case with solid metals that accumulate crystalline defects the more they are deformed. The properties of LMs are highly favorable for stretchable electronics, in which low and stable electrical resistance are needed under repeated mechanical deformation. In fact, several studies on LM-composites have shown a moderate increase in resistance R relative to the initial resistance (R_0) of $R/R_0 \approx 1$ under high mechanical strain (0–100%).[62,63]

3. Methods to Pattern LMs

We organize this section by categories of approaches to pattern LM.[64,65] These approaches typically involve one or more of the strategies to pattern liquids depicted in Figure 1. In each subsection, we describe the capabilities and limitations of the methods. This is not intended to be a comprehensive review, but rather a summary of key concepts, advances, and opportunities.

3.1. Injection

One way to physically constrain LM within a desired shape is by injecting the fluid into a container. Examples include elastomeric microchannels, hollow polymer fibers, and cavities in 3D printed plastics. Refs. [46,70] feature some of the earliest reports of injection filling of LM into microchannels. **Figure 3**a shows the concept of injection. To inject a liquid is to literally force it within a confined space, which requires a pressure differential that can be applied with a syringe. The container should have a pathway for displaced air to escape. The applied pressure differential must be sufficient to break the oxide layer. To a first approximation, the pressure differential, P, across the interface follows the Laplace equation, as shown in Equation (1).

$$P \approx 2\gamma \cos\Theta / R \tag{1}$$

In Equation (1), the effective interfacial tension, γ, is complicated because the surface of the metal has two interfaces (metal/oxide and oxide/air) plus a ≈3 nm-thick shell of solid oxide. Thus, the term "effective tension" is used to capture this complexity. The oxide must be broken continuously to induce the metal to flow in the presence of oxygen. Rheological measurements report the value necessary to break the oxide to range from ≈0.3–0.5 N m^{-1}.[20,46] In Equation (1), R is the radius of curvature, which is approximately the radius of the cross-section of the channel. This equation assumes the container (e.g., microchannel) has round, cylindrical walls and a contact angle θ, which is typically large (≈150°). Equation (1) suggests that filling a channel that is 10–20 μm in diameter will require ≈1 atm of gauge pressure. Likewise, Equation (1) predicts that filling channel 1–2 μm in diameter will require ≈10 atm of gauge pressure.

Once the LM is injected, it naturally stays within the channels due to the stabilizing effects of the oxide layer. In most cases, the oxide forms on all LM interfaces. For example, materials such as silicones, which are highly permeable to oxygen, are commonly used for microfluidics. The permeability ensures that oxide forms on any exposed metal, including metal in contact with the silicone walls.[46] In contrast, mercury—which does not rapidly form an oxide[71]—can be injected into microchannels, but it rapidly withdraws from the channels due to capillary forces.[46] After injecting the LM, the inlet and outlet can be sealed (e.g., with silicone) to prevent leakage. If needed, additional wiring can be connected to the LM before sealing the holes to provide electrical connections.

LM can be used to "metallize" a variety of microchannels, cavities, fibers, and parts. Typically, microchannels are formed by molding silicone against a topographical mold and then sealing the replica against another layer of silicone. Hollow

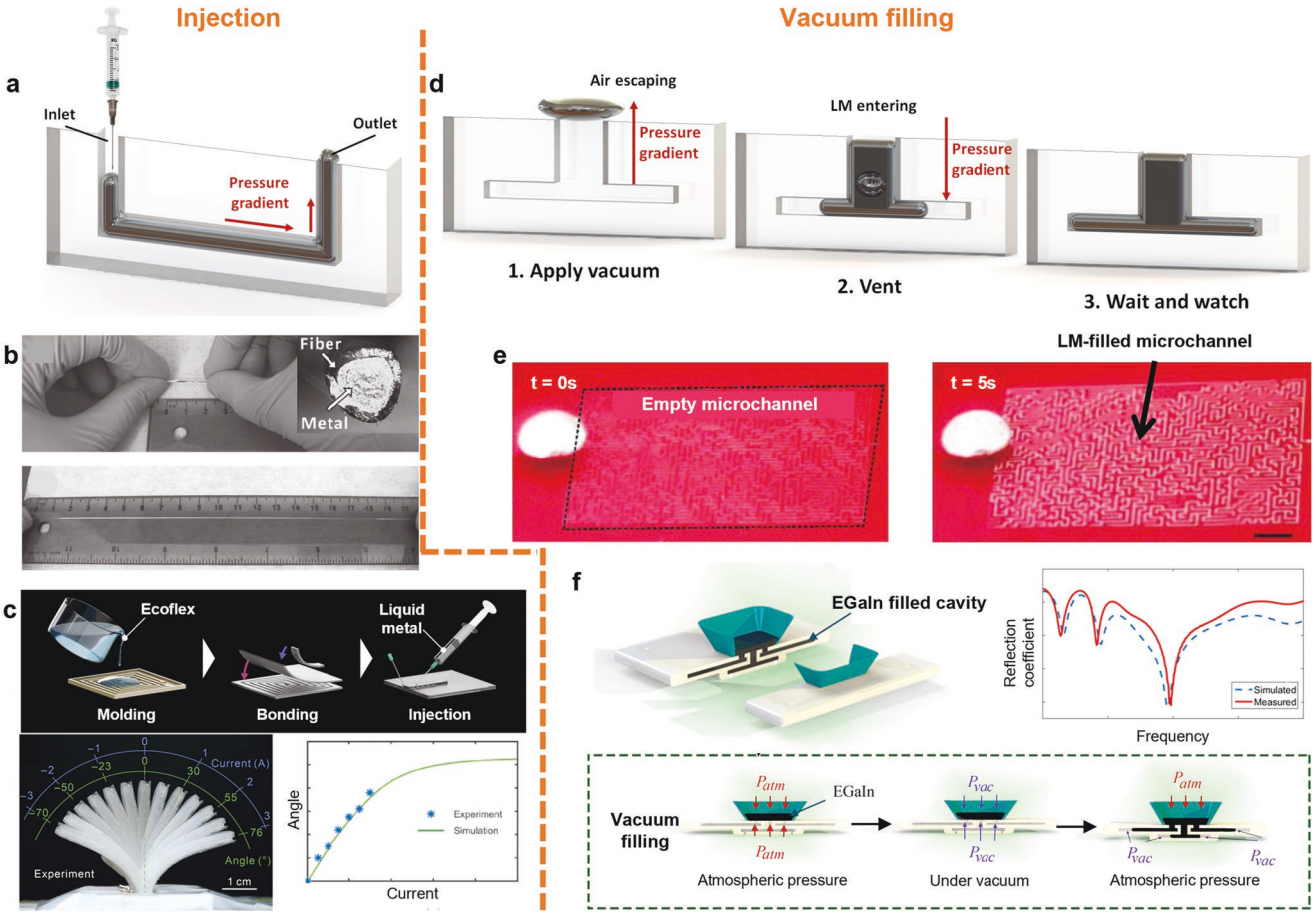

Figure 3. Injection of LM into microfluidic "containers" a) To fill a microchannel with LM by injection, an inlet and at least one outlet are necessary. A pressure gradient breaks the oxide and pushes metal into the channel while displacing air to the outlet(s). b) Hollow elastomer fibers injected with LM could remain electrically conductive even while being stretched and twisted.[66] c) Soft electromagnetic actuators made by injecting LM into coil-shaped Ecoflex elastomer microchannels.[67] d) To vacuum-fill a microchannel with LM, only one opening is necessary. First, LM should be deposited over the opening, covering it entirely. When the pressure outside the sample is reduced, air within the channel will vent by bubbling through the LM puddle or diffusing through the walls of the channel. After removing the air within the channel, increasing the pressure outside the sample causes the LM sitting on the opening to flow into the channel and fill it to its edges. e) Vacuum-filling is particularly suitable for filling channels with complex designs and fine features.[68] f) LM can vacuum-fill cavities in 3D printed parts for metallization of plastics. Here, the metal serves as a functional antenna.[69] b) Reproduced with permission.[66] Copyright 2013, Wiley-VCH. c) Reproduced with permission.[67] Copyright 2020, American Association for the Advancement of Science. e) Reproduced with permission.[68] Copyright 2017, Royal Society of Chemistry. f) Reproduced with permission.[69] Copyright 2017, Elsevier.

fibers and capillaries are available commercially. Stretchable fibers with customized internal structure and composition can be achieved by elegant thermal drawing techniques that avoid the need for injection.[72,73] It is also possible to inject LM into cavities and channels within 3D printed parts (cf. Figure 3f).[60]

As an example of injection, Figure 3b shows stretchable, conductive wires consisting of LM injected into hollow elastomer fibers.[66] The LM maintains metallic conductivity between the ends as the fiber stretched up to ≈700%, which was the failure point of the polymer shell. Recent studies have demonstrated conductivity to strains of 1800% by using other polymers.[74,75] As LM has low viscosity and flows readily in response to applied stress, the mechanical behavior of the LM-filled tube and the hollow tube were effectively the same, although in some cases the LM can enhance the mechanical properties (e.g., toughness).[76 77] Such fibers can be strain-cycled many thousands of times without hysteresis.

Figure 3c shows another example of injection: soft electromagnetic actuators consisting of LM-filled coil-shaped microchannels made of a commercial silicone elastomer.[67] By passing electrical current through the conductive LM coils, a magnetic force that is orthogonal to the plane of the coil is produced, which causes the soft elastomer to deform, as depicted in the photo (Figure 3c).

There are several drawbacks of injection. It requires cavities, which must be fabricated prior to injection. Wide or extremely soft structures are difficult to pattern by injection due to the risk of channel collapse. Injection requires an inlet and outlet port,[78,79] which may result in undesirable features of LM in the final structure and makes it difficult to pattern dense, isolated features. The need to apply larger pressures to fill smaller channels can lead to leakage or device failure.

Most of these limitations can be addressed using vacuum filling. Figure 3d shows the principle of vacuum-filling, which

was first described for aqueous solutions[80] and then later demonstrated for LMs.[68] First, LM is placed over the inlet(s), completely covering all the openings of the microchannel. Then, the entire structure is placed in a vacuum chamber, which forces the air within the microchannel to bubble out through the LM and permeate through the microchannel walls. Returning the chamber to atmospheric pressure produces positive pressure relative to the vacuum inside the channels. This pressure differential pushes the LM sitting on the inlet(s) into the microchannels with dimensions as small as 5–10 μm.

Compared to injection filling, vacuum filling results in more thorough filling of LM into the microchannels.[68,81,82] Vacuum filling can pattern complicated patterns (e.g., dead end mazes, coils, circuit board lines) by eliminating the possibility of trapping air inside the channels (Figure 3e).[68] Unlike injection filling, no outlet is required. The approach is completely hands-free and avoids the leakage problems associated with injection since the pressures inside the channels are always below atmospheric pressure.

Vacuum filling is not without limits. Although the filling occurs rapidly (1–10 s), in our experience the vacuum chamber step requires tens of minutes to remove the air when using a simple roughing pump to evacuate the chamber. The vacuum filling technique also requires an inlet with a continuous fluid path to the features. Thus, it cannot be used for arbitrary geometries. Nevertheless, it can be used to metallize closed-end features, such as those in 3D printed parts.[69]

Figure 3f shows an example of 3D printed thermoplastic parts with hollow cavities. The cavities can be filled with LM using vacuum filling. In this example, the metal forms an antenna structure within the 3D part that has spectral properties that agree with theory.[69]

Once inside channels, LM adheres to the walls due to the oxide. In some cases, it may be preferable to withdraw the metal after it has been injected. The adhesion can be avoided, in principle, by working in an oxygen-free environment, but in practice it is very difficult to remove enough oxygen to prevent surface oxidation. The oxide can be removed using strong acids (1 M HCl) or base (1 M NaOH), but this may also be undesirable in many applications due to the use of extreme pH solutions. Likewise, lubrication layers (e.g., slip layers) of water or other fluids can form a thin layer of liquid between the oxide and walls to avoid adhesion.[38,83] Furthermore, the oxide can be chemically modified[84] (e.g., with silanes or phosphates anchored to the hydroxyl groups on the oxide) to help minimize adhesion.

A more practical way to avoid adhesion of the oxide to the walls of the channel is to use surface roughness. Surface roughness prevents good oxide contact to the substrate (explained in Section 2).[43–45] While roughening the interior walls of small channels is challenging, it is possible to deposit particles on the inside of thermoplastic microchannels to prevent adhesion, thereby allowing LM to be injected and withdrawn without leaving residue on the walls.[60]

3.2. Direct Writing

Direct ink writing is a general term that captures a wide range of additive techniques that dispense materials such as inkjet printing or extrusion 3D printing.[49,82,85–86,88–96] Early demonstrations of additive patterning of pure LM at ambient conditions used nozzle based printing.[50] Dispensing LM out of a nozzle results in a spherical structure due to interfacial tension. These droplets can be stacked on a substrate, as shown in **Figure 4**a.[85,92] The droplets undergo arrested coalescence upon contact (cf. Figure 2b). The exact fate of the oxide at the interface between the droplets is unknown, but efforts to pull the drops apart show that they make continuous metal–metal contact.[50,97] Although it is remarkable to be able to create structures up to ≈1 cm tall using this approach stabilized by a ≈3 nm oxide layer, the resulting structures can easily topple over or smear in response to vibrations or stress. Thus, they are typically encased in elastomer after printing to create stretchable conductors, such as the electrical interconnect between LEDs shown in Figure 4b. Conjoining droplets is not a very fast approach to patterning due to its serial nature. Thus, additional considerations must be made to direct write LM.

To avoid dispensing spherical droplets of metal, direct writing LM relies on adhesion between the oxide skin and the substrate. The adhesion shears the metal from the nozzle as it translates relative to the stage.[49,82,89,90] This approach to printing has similarities to writing with a ballpoint pen: liquid does not come out of the pen until it is sheared across a "wetting" substrate. Thus, printing occurs at dispensing pressures way below that required for extrusion. The oxide skin that forms on the printed LM is effectively a "container" that holds the shape of the printed structure. The diameters of the printed structures are similar to the nozzle diameters; remarkably, structures with diameters as small as ≈2 μm have been printed using this approach (from a nozzle diameter of 5 μm), as shown in Figure 4c.[85]

A downside of this direct-write approach is that it requires surfaces with good adhesion (i.e., smooth surfaces) and excellent control of the distance between the nozzle and substrate.[92] Just as it is difficult to write on certain non-wetting surfaces using a ballpoint pen, adhesion between the oxide skin and the substrate is crucial for direct writing of LM. Advancing and receding measurements show LM droplets adhere to nearly all smooth surfaces.[40] Yet, such measurements expand droplets against a surface, and may not be representative of the contact between the LM meniscus at a printing nozzle and a substrate. Thus, a "peck test" was introduced to evaluate a substrate's compatibility for direct writing LM;[49] the LM meniscus on the tip of a nozzle touches or "pecks" various surfaces 100× (Figure 4d). If the adhesion is sufficient such that a small LM droplet gets deposited on the substrate after the brief contact, then the surface is likely suitable for direct printing. For example, Figure 4d shows substrates that pass (left image) and fail (right image) this test. The "peck test" is a practical tool as it is quick and easy to conduct, and the outcomes are clear-cut (pass/ fail) and simple to interpret. These measurements show that LM prints well on hydrophilic substrates (e.g., glass or silicon wafers) and plasma treated silicones, presumably due to hydrogen bonding with the oxide. Adhesion can be promoted during printing "on demand" by applying a voltage to the LM relative to a sub-surface electrode to generate electrostatic stresses, although this approach does require a sub-surface electrode.[93]

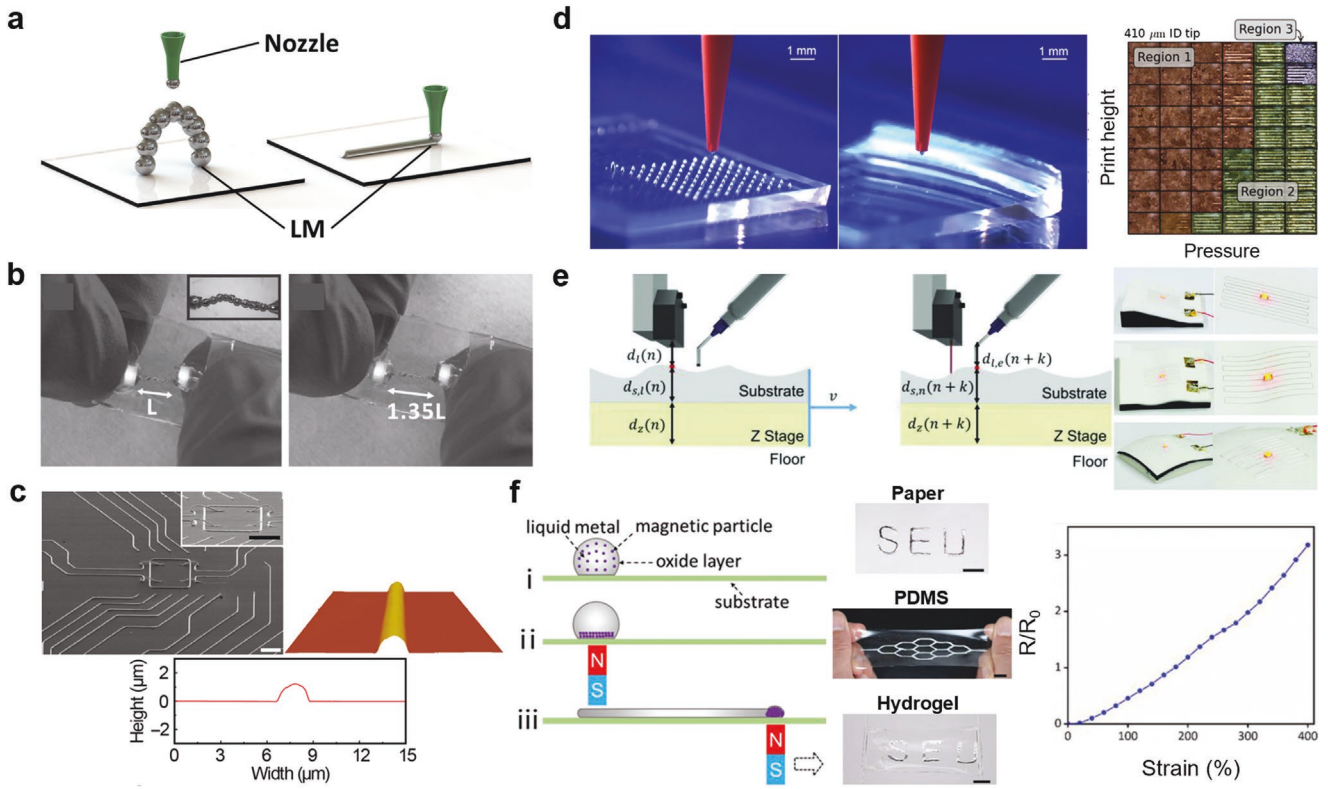

Figure 4. Direct-write printing of LM. a) Left: Printing of self-supporting 3D LM structures by stacking droplets. Right: Direct writing of LM by shearing it from a nozzle. b) Connected LM droplets embedded in an elastomer form stretchable interconnects.[50] c) SEM image and AFM profile of high resolution printed LM traces.[85] d) Left: "peck test" of LM to identify good and bad surfaces for printing. Right: Printability of LM according to nozzle pressure and printing height.[49] e) Direct writing of LM on uneven surfaces using a laser to control the nozzle-substrate gap.[86] f) Using a magnet to drag LM containing magnetic particles.[87] b) Reproduced with permission.[50] Copyright 2013, Wiley-VCH. c) Reproduced with permission.[85] Copyright 2019, American Association for the Advancement of Science. d) Reproduced with permission.[49] Copyright 2019, Wiley-VCH. e) Reproduced with permission.[86] Copyright 2019, Wiley-VCH. f) Reproduced with permission.[87] Copyright 2019, Wiley-VCH.

The combination of the size of the nozzle, dispensing pressure, and distance between the nozzle and the substrate ("print height") is important, as recently reviewed.[96] Briefly, Figure 4d shows printed structures as a function of the print height and nozzle pressure. In region 1, the meniscus of metal at the nozzle does not make good contact and therefore LM does not print. In region 3, the pressure is too high and LM is being dispensed too fast for the given stage speed. In region 2 (modest pressure, and small print height), the LM prints well. This underscores the importance of controlling the distance between the nozzle and substrate, which is easiest if the substrate is flat. It is possible to direct write LM on uneven surfaces by using a laser sensor to measure and maintain the distance between the nozzle and the surface in real-time (distance d in Figure 4e).[86]

Lastly, it is possible to use magnets to manipulate the motion of LM without the use of a nozzle (Figure 4f).[87] Gallium is diamagnetic, but it is possible to mix magnetic particles into the LM to make it responsive. Moving a magnet below a substrate of interest drags (shears) the LM mixture across the surface, leaving behind a metal trace due to the adhesion of the oxide to the substrate. A drawback of this approach is the low resolution (500 μm) since the metal is not confined by the nozzle.

3.3. Stencil Printing

In this section, we consider stencil-based patterning of LM, which takes advantage of the fluidity of the LM and the ability of the oxide to adhere to surfaces to replicate the stencil pattern. There are several variations of stencil-based patterning, but in general, they have the following components in common: i) ink, ii) substrate, iii) stencil, and iv) tool(s) for forcing the ink through the openings in the stencil.

At its most basic level, stencil printing can be done by placing the stencil on the substrate, then using a squeegee or roller to spread a puddle of LM over the stencil, as shown in **Figure 5**a. The fluidity allows the ink to pass through the openings and the oxide helps it adhere to the substrate.[98–109] Peeling the stencil off leaves a pattern of LM on the substrate. Since the stencil is reusable and the process is quick and easy to automate, stencil printing has gained popularity. Stencils can be created easily using xurography (cutting with a craft cutter) or laser cutting, for example.

Stencil printing resolution is defined, in principle, by the size of the opening in the stencil. Typically, the stencil is made of a sheet of polymer, metal, or ceramic, and is about 100–200 μm-thick. To deposit finer features, the thickness of the stencil (and by relation, its total sidewall area) should be

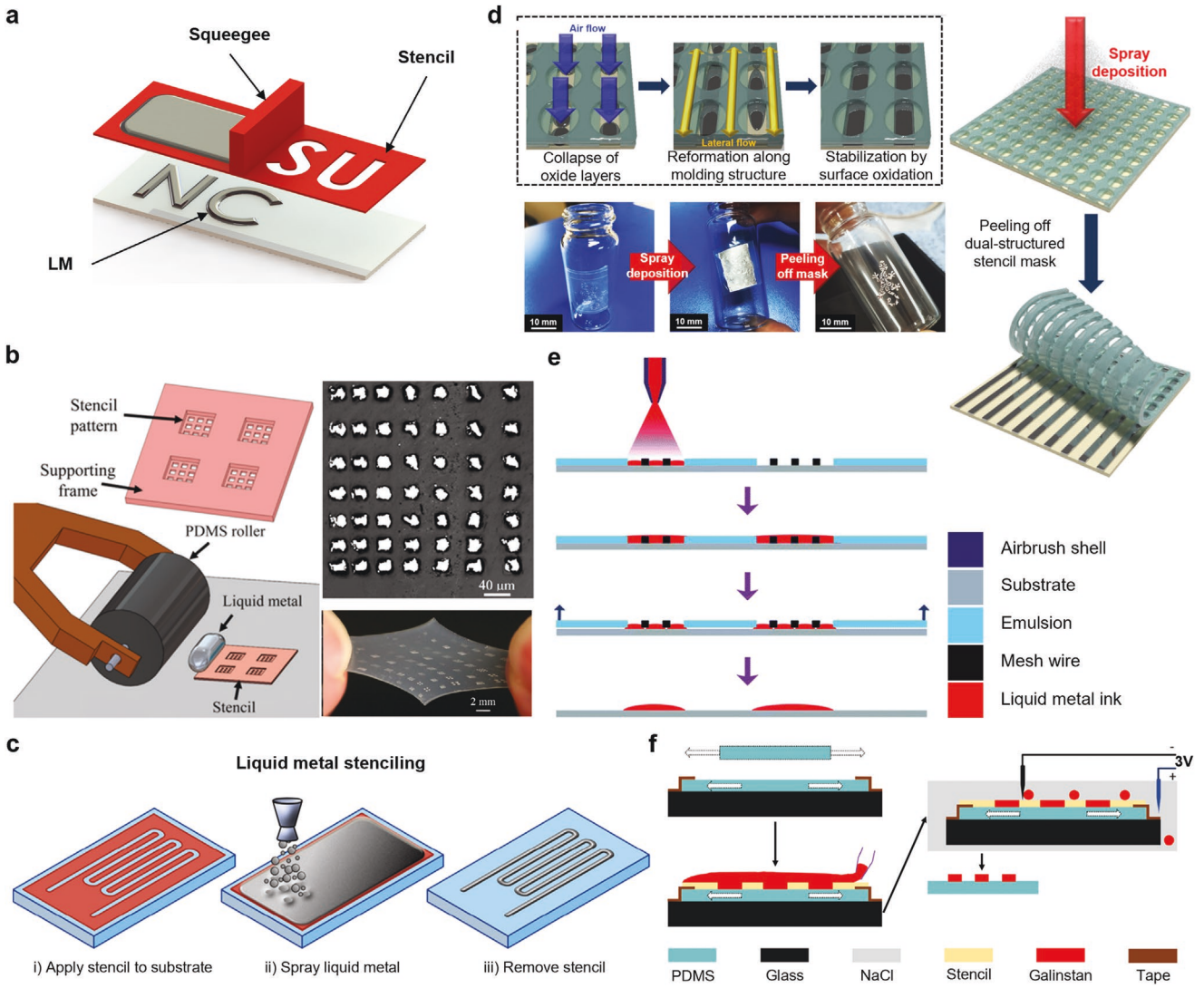

Figure 5. Patterning of LM using stencils. a) Schematic of the general process of stencil printing. A squeegee or roller pushes LM into the openings of a stencil placed temporarily on a target substrate. b) The resolution of LM patterns can be improved by using thinner stencils. Here, a thin 3 µm metal stencil supported by a thicker frame layer produced LM features as fine as 10 µm.[98] c) Spray deposition of LM on a polymer stencil.[99] d) Patterning LM using a double-layered polymer stencil. The top layer with larger holes serves as a supporting frame for the bottom stencil. This kind of stencil structure enables the deposition of hollow shapes and disconnected islands.[100] e) Screen printing of aerosolized LM. Due to its large surface tension, it is necessary to spray the LM so that it can pass through the narrow apertures of the mesh.[101] f) Applying a reducing potential to the excess LM on top of the stencil causes it to bead up for easy removal.[102] b) Reproduced with permission.[98] Copyright 2017, American Chemical Society. c) Reproduced with permission.[99] Copyright 2021, MDPI. d) Reproduced with permission.[100] Copyright 2020, Wiley-VCH. e) Reproduced with permission.[101] Copyright 2015, Royal Society of Chemistry. f) Reproduced with permission.[102] Copyright 2019, IOP Publishing.

reduced. Unfortunately, the thinner the stencil, the flimsier it becomes, which makes it tedious to handle without buckling, tearing, or breaking. Thus, it is necessary to reinforce the stencil so that it can be thin and strong. For example, by adding a supporting layer to frame the pattern on the stencil without obscuring it, the stencil can be made sturdier.[98,100] One approach, shown in Figure 5b, is to use a multilayer copper structure composed of a 3 µm-thick copper stencil on 30 µm-thick supporting frame by photolithography and electroplating. This approach produced LM prints as narrow as 10 µm, which is one order of magnitude smaller than previously reported LM stencil prints. It was reported that the stencil became very fragile when it contained an aperture longer than 1 mm. Thus, there are opportunities to develop high resolution stencils with the right mechanical properties to accommodate fine and long features.

Another difficulty in stencil printing LM is trying to completely fill the openings in the stencil. Pushing LM into small geometries—such as corners—requires sufficient pressure to overcome interfacial forces, yet the ability of low viscosity LM to flow along the "path of least resistance" means it is prone to go elsewhere during the squeegee process. These properties often result in printed structures with "line edge roughness" (for example, see the irregular features in Figure 5b).

"Atomization" of LM—i.e., pneumatically spraying LM from a nozzle to form droplets—has been adopted as a tactic to mitigate this issue as tiny LM droplets can travel directly into tight corners without facing the interfacial resistance of the bulk metal.[110,111] In one of the earliest reports[111] of using this approach to stencil pattern LM, the lateral feature size achieved was in the 100 s μm range. Furthermore, the LM aerosol can easily be produced using a simple pneumatic atomization apparatus and sprayed onto large areas quickly, as shown in Figure 5c.[99,104,106–108] Despite oxidizing in midair, the aerosol of particles coalesce into a conductive film upon impact with the substrate.[99] The resulting structures still have line edge roughness, due in part to the metal adhering to both the substrate and the stencil as the stencil separates from the substrate.

Flexible and elastic polymer stencils are helpful for patterning LM on curved surfaces. However, the critical force to cause buckling in polymers is much lower than that of stiffer materials like metals and ceramics. A stencil with dual-thicknesses can solve this problem (Figure 5d).[100] Patterning the top side with relatively large holes (≈20 μm in diameter) allows LM through, while the side that contacts the substrate contains smaller stencil features. For a stencil design consisting of narrow, parallel lines, the polymer stencil was able to remain stable without buckling or lateral collapse down to 30 μm width and spacing and length of 800 μm. Unlike regular stencils, this type of double layered stencil can accommodate disconnected islands and hollow shapes (like the white portion inside the letter "B") due to the structural continuity offered by the support layer (which is akin to the mesh used in screen printing).

Screen printing is similar to stencil printing, but differs in the use of a mesh that covers the entire stencil including the openings. Whereas stencils usually conform intimately to the target substrate, screens used in screen printing only contact the substrate when the squeegee passes across the screen. Despite the popularity of screen printing for industrial printing, it is difficult to screen print LM. The mesh size of a silk screen is usually small (<100 μm), which makes it challenging for high surface tension LM to penetrate these openings using the modest pressures applied by a squeegee (cf. Equation (1)). For LM to be able to pass through the mesh apertures, it has to be broken up into tiny droplets smaller than the size of the opening, which can be accomplished by spray depositing atomized LM (as shown in Figure 5e).[101]

One technique to improve the resolution of stencil printing takes advantage of pre-strained substrates. As illustrated in Figure 5f, a prestrained silicone substrate is UV ozone-treated to improve adhesion with LM.[102] The LM is then cast over the stencil. The excess LM is removed by first immersing the silicone substrate and stencil mask in salt water solution. Applying a reductive potential to the metal removes the surface oxide layer.[112] Subsequently, the excess LM dewets the stencil and removes easily. Upon releasing the strained silicone, the width and spacing of the LM wires decrease by ≈1.5×, proportionate to the amount of prestrain. This resulted in LM wires with <30 μm widths.

Although stencil printing and spraying LM is simple and therefore attractive, there are drawbacks: i) Unlike injection and DIW, the LM will get on surfaces other than the intended pattern. ii) The clean-up process of removing and recycling the excess LM left on the stencil can be messy and time consuming. In addition to electrochemical reduction of the oxide,[102] immersing the stencil in acid or base solution can remove the oxide that otherwise adheres the LM to the stencil. More recently, an approach that involves the use of a spin-coater for stenciling LM has been demonstrated and the authors report that the centrifugal force from spinning helped to remove the excess LM.[113] iii) The surfaces and edges of the spray deposited pattern are often uneven. iv) A resolution of hundreds of micrometers is easy to obtain and can improve to tens of micrometers using best practices.

3.4. Selective Adhesion

One way to pattern a liquid is to take advantage of its preferential adhesion or wetting to regions of a surface (Figure 1b).[117–121] The interfacial behavior of LM depends on whether the metal is bare or coated with its native oxide. We discuss the selective wetting of bare LM in Section 3.6 and focus here on LM with the oxide.

When coated with its native oxide, LM adheres to nearly all smooth surfaces (when it is volumetrically advanced against a substrate).[40] However, it does not adhere to rough surfaces due to poor contact between the oxide layer and the substrate, as illustrated in **Figure 6**a.[40,44,122–125] Such surfaces may be called "metallophobic" (in an analogous term to "hydrophobic"), but that is a bit of a misnomer because of the presence of the oxide between the metal and substrate. In the absence of the oxide, the bare metal has a large interfacial energy and does not wet most surfaces. There are two exceptions: 1) bare LM wets metal surfaces via "reactive wetting" due to metal–metal bond formation (covered in Section 3.6), and 2) LM can wet certain reentrant surfaces.[126]

Figure 6a shows a strategy to take advantage of selective adhesion of the oxide-coated LM to smooth regions surrounded by an otherwise rough surface. This strategy was implemented to metallize a 3D printed object by manipulating the roughness on different areas of the surface (Figure 6b).[60] The photocured resin (polymethyl methacrylate, PMMA) was coated with fumed silica to roughen the surface. Regions of the coating were ablated using a commercial laser engraver. LM adhered to only the ablated (smoother) surface.

Alternatively, a metallophobic (rough) surface can be selectively smoothed to pattern LM by selective adhesion.[114] Figure 6c shows that a polymethacrylate (PMA) glue patterned (by hand or printer) on a rough piece of paper effectively fills the gaps and reduces the local roughness of the paper. Furthermore, functional groups on PMA may help adhere to the oxide. LM applied and removed to the paper adheres only on the glue traces. This method achieved 300 μm features. The paper is flexible and foldable, and the LM traces did not lose electrical conductivity even after folding. Note that while LM adheres poorly to fibrous substrates, surprisingly we found that small LM particles have excellent adhesion to individual fibers of a fabric, which warrants further study.[127]

Due to the excellent adhesion of the native oxide to substrates, it is often difficult to transfer LM traces to other surfaces since it undergoes cohesive failure. That is, the force applied to pull LM features from a surface breaks the thin

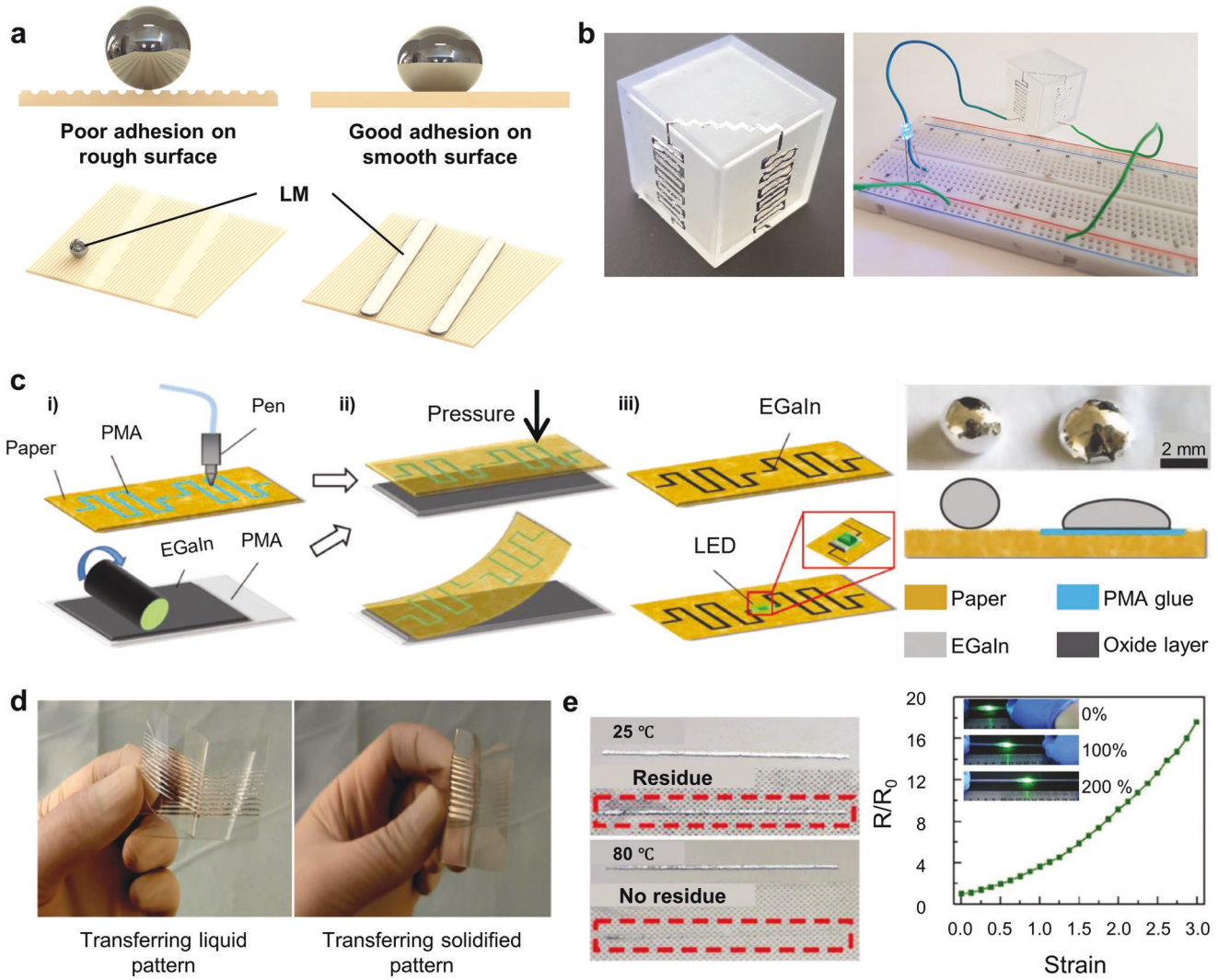

Figure 6. Patterning methods based on selective wetting/dewetting/adhesion of LM featuring a native oxide. a) Left: poor adhesion between LM and a rough surface ("metallophobic surface"). Right: LM adheres to a smooth surface facilitated by its native oxide. b) Preferential wetting of LM on smooth portions of a 3D printed cube with an otherwise rough surface.[60] c) LM native oxide adheres to PMA glue, but not rough paper. The LM pattern deposited on the PMA is electrically continuous and can be used to make circuits.[114] d) Solid metal features transfer cleanly to an elastomer from a polymer sheet without cohesive failure experienced when the metal is liquid.[115] e) A LM composite pattern can be cleanly transferred from a PVA-fructose film onto a silicone film by heating as the adhesion of the LM composite on fructose weakens at elevated temperature.[116] b) Reproduced with permission.[60] Copyright 2021, American Chemical Society. c) Reproduced with permission.[114] Copyright 2018, Wiley-VCH. d) Reproduced with permission.[115] Copyright 2015, Wiley-VCH. e) Reproduced with permission.[116] Copyright 2019, Wiley-VCH.

oxide at the oxide-air interface rather that peeling it from the substrate. Freezing the metal stiffens the bulk of the metal. By casting elastomer over it, it is possible to detach the metal from the substrate, as shown in Figure 6d.[115,128]

Increasing the temperature of some surfaces can weaken the adhesion between LM oxide and the surface (Figure 6e).[116] For example, the adhesion between LM and fructose patterns weakens at elevated temperatures (≈80 °C), which facilitates transfer of LM patterns onto other stretchable substrates.

Limitations of these adhesion-based approaches for patterning includes 1) the need to pre-pattern adhesive versus non-adhesive regions on a surface, and 2) the need to have sufficient contact to make adhesion, which limits the resolution (in practice) to hundreds of micrometers.

3.5. Rheological Modification

3.5.1. Composite Conductors using LM as the Continuous Phase

Rheological modification is one way to change the behavior of liquids to better control the shape (c.f. Figure 1d). As shown in **Figure 7**a, dispensing pure LM from a nozzle results in droplets. The ability to modify the rheology to form a paste can allow direct extrusion of LM from a nozzle, as shown on the right side of Figure 7a. The rheology modifier could be metallic particles, nonmetallic particles, entrained flakes of the native oxide, other fluid phases, or combinations of two or more of the above.

Figure 7b shows one of the earliest examples of printable pastes. This example mixed nano- and micro-sized nickel particles

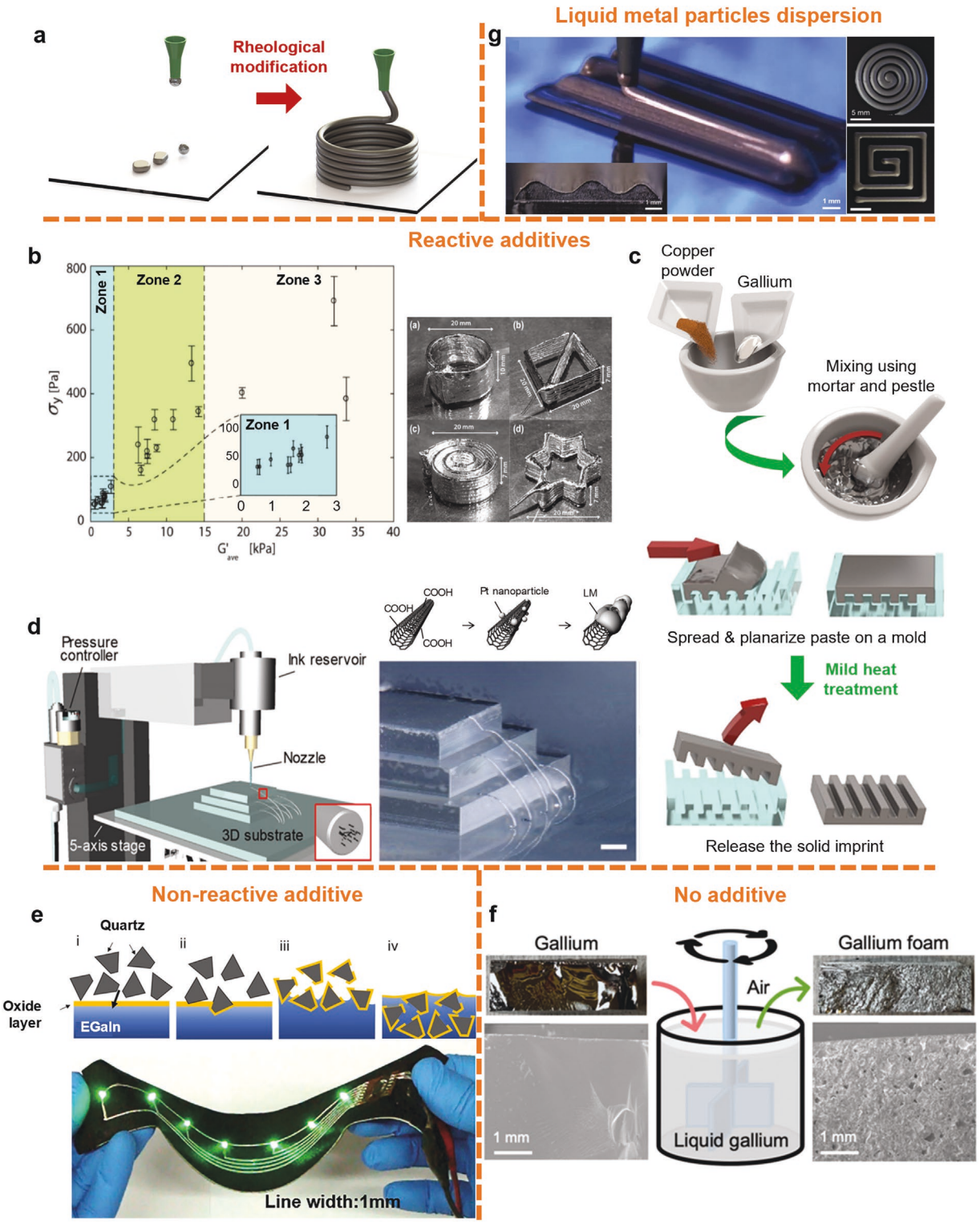

Figure 7. Rheological modification of LM for patterning. a) Left: LM comes out from a nozzle as droplets. Right: The rheologically-modified LM comes out as a stable filament. b) LM paste containing Ni particles enables 3D printing.[129] c) LM pastes containing Cu particles can be directly printed, or imprinted, then the metal solidifies by forming $CuGa_2$ intermetallic.[130] d) Printable CNT/LM composite that can form spanning wire bonds.[131] e) Quartz particles/LM composite with mixing mediated by the oxide layer. The composites were stencil printed.[132] f) Optical and SEM images of Ga/Ga-oxide composites formed by simply stirring LM.[133] g) Direct writing LMP–polymer composite (left, scale bars: 1 mm). Square and circular spiral pattern of LMP–polymer composite printed by direct writing (right, scale bars: 5 mm).[134] b) Reproduced with permission.[129] Copyright 2018, Wiley-VCH. c) Reproduced with permission.[130] Copyright 2020, American Chemical Society. d) Reproduced with permission.[131] Copyright 2019, American Chemical Society. e) Reproduced with permission.[132] Copyright 2020, American Chemical Society. f) Reproduced with permission.[133] Copyright 2020, Royal Society of Chemistry. g) Reproduced with permission.[134] Copyright 2020, Royal Society of Chemistry.

into LM by sonication at ambient conditions to produce pastes with higher viscosity (resistance to flow), yield stress (structural strength), and storage modulus (which relates to structural stability) relative to pure LM.[129] However, only certain compositions print well. Figure 7b provides guidelines for printing based on the yield stress and storage modulus of the paste. Pastes with very low yield stress (σ_y) and storage modulus (G') were not printable because they lacked the structural rigidity to be shaped (labeled as "zone 1" in Figure 7b). On the other hand, composites with exceptionally high σ_y and G' (zone 3 in Figure 7b) were too stiff to be extruded. The optimal σ_y and G' for extrusion printing were determined to be about 100–400 Pa and 3–15 kPa, respectively (zone 2 in Figure 7b), resulting in filaments upon extrusion. Such filaments can be stacked to form multilayered 3D structures as shown on the right side of Figure 7b. The electrical conductivity of the pastes was comparable to that of pristine LM, despite the inevitable increase in oxide content resulting from the intense shearing of the LM in air during mixing.

Due to the high cohesive energy of LMs, it is generally energetically unfavorable to mix particles into LM without the aid of LM native oxides.[135] Metal particles serve as the exception since they can form metal–metal contact with LM to produce pastes. Yet, in practice, many metal particles contain surface ligands or native oxides that limit the ability to create metal–metal contacts. Removing these surface "contaminants" can make mixing easier as shown in Figure 7c, in which Ga mixes readily after cleaning the Cu in a reduction furnace. Such all-metal pastes can be patterned by direct printing and molding (Figure 7c). In addition, the interaction between LM and other metals eventually lead to solid intermetallics such as $CuGa_2$, thus allowing the printing of solid metals using room temperature pastes.[130]

Non-metallic fillers, such as carbon nanotubes (CNT) normally would not mix readily into LM. Yet, decorating the CNTs with platinum (Pt) nanoparticles enables favorable metal–metal contacts with the LM to facilitate mixing. The inclusion of CNTs effectively increases the rigidity and structural stability of the printed features. Figure 7d shows the fine 3D printed "bridging" wires produced by extruding the composite through a narrow glass nozzle (diameter 5–140 μm) using pneumatic pressure.[131] A downside of this approach is the added step of decorating CNTs with Pt nanoparticles.

Alternatively, non-metallic inclusions can be incorporated into LM using the LM native oxide to mediate mixing. The native oxide behaves like a surfactant since it is more energetically favorable for the LM to interface with its own oxide instead of directly touching the foreign phase (refer to Section 2). As shown in Figure 7e, the native oxide can encapsulate quartz particles during mixing to form a LM paste. The resulting paste has higher viscosity and yield stress compared to pristine LM, which enables it to be patterned into lines using a stencil with wide (1 cm) apertures. It is possible to separate the LM from the particle fillers by removing the oxide using acid or base due to the chemically-inert nature of quartz particles in LM.[132]

It is also possible to form a paste consisting only of LM and its native oxide by simply stirring LM in the presence of oxygen. The stirring generates excess oxide "flakes" that get dispersed throughout the bulk of the fluid.[133] Figure 7f shows a foam formed by entraining oxide and air into the LM, which increases the viscosity and storage modulus relative to pure LM. The ability to tune the rheology of LM without introducing additional foreign particles could enable printing and be beneficial for multiple reasons including eliminating sedimentation due to density differences, cutting costs, and minimizing unwanted intermetallic formation at interfaces between LM and particles.

The aforementioned mixing approach can be used to incorporate ferromagnetic neodymium–iron–boron microparticles in EGaIn, which not only makes it respond to magnetic fields, but also alters the rheology of the mixture.[136] Magnetization increases the storage modulus and viscosity of the ferromagnetic LM mixture by ≈3 orders of magnitude. In addition to exhibiting reversible magnetization, the ferromagnetic LM putty could be pressed into a shape and then reshaped, like modelling clay. Less viscous LM mixtures with lower concentration of ferromagnetic particles could be dispensed from a nozzle to direct write conductive and magnetically responsive patterns.

There are several challenges and opportunities for improvement with the rheological modification approach for patterning. It is difficult to make uniform pastes by mixing particles (often surrounded by crumpled oxide flakes) into a low viscosity liquid. Buoyancy effects can also result in non-homogenous mixtures, as can agglomeration. Non-homogeneous pastes do not dispense uniformly from a print nozzle; the low viscosity LM tends to flow out more readily than the solid particles. In addition, the shelf-life of pastes may be limited due to the reasons above as well as the ability of LM to form intermetallic phases with metallic fillers. Non-metallic fillers can be inexpensive and offer useful properties (e.g., lower density), yet they can decrease some of the desirable metallic properties of pastes relative to pristine LM.

3.5.2. Dispersions of Liquid Metal Particles

Breaking bulk LM into small droplets within another fluid is another approach to drastically alter the rheology of LM to make it easier to dispense and pattern. This can be done using common mixing equipment such as a planetary mixer, sonicator, and vortex mixer or even by manual stirring.[137] The continuous phase of the mixture may be a viscous polymer melt, uncured elastomer mixture, or pre-gel solution that is intended to solidify or set as the composite matrix, securing the LMPs in place. Alternatively, LMPs can be dispersed in a volatile liquid (e.g., ethanol) that serves as a carrier fluid for the deposition step, but is later supposed to vaporize and leave a pasty film of LMPs on the substrate. The resulting individual LM particles will be coated in native oxide and can range from micro- to nano-sized.

This method of rheological modification[134,138] enables LM particle dispersions to be deposited by direct write printing, stencil printing, and even inkjet printing.[52,134,139,140] At high loadings, the presence of the LM particles in a fluid can significantly alter the rheology relative to the pure fluid. For example, silicone pre-polymer is Newtonian, but silicone pre-polymer

with LM particles can have shear thinning behavior, which is ideal for printing.[134] Figure 7g demonstrates direct printing of the LM–silicone composite into 400 μm-wide lines. Due to its high storage modulus, the composite with 90 wt% LMPs can be printed into multilayered wires. A recent study shows that by adjusting the printing speed, the aspect ratio of LM inclusions within such direct write-printed composites can be tuned.[138] For polymer matrices (such as silicone pre-polymer), the composite can be cured after deposition to secure the shape. If the carrier fluid is a volatile liquid (e.g., IPA, ethanol), it can be vaporized after the mixture has been deposited, leaving behind a layer of LMPs in the desired shape.

As-prepared LM particle dispersion composites are generally not electrically conductive since LM is not the continuous phase. Non-conductive LMP composites can be useful for dielectric applications since dispersion of LMPs increases the effective dielectric constant of the composite.[52,141–143] Likewise, they are good for increasing thermal conductivity of a stretchable composite.[55] Otherwise, conductive pathways can be activated within the composite by "sintering" LMPs along selected paths using various techniques (discussed in Section 3.6).[51,52,134,139,140] Alternatively, there are "tricomponent" LMP dispersion inks that include another conductive inclusion phase (e.g., silver flakes) in addition to the LMPs within the polymer binder. Such composite inks exhibit $\approx 10^3$ S m^{-1} conductivity when stretched (a less targeted type of mechanical sintering).[144,145]

3.6. Other Patterning Techniques

In this section, we discuss LM patterning techniques that do not neatly fit into the specific categories of methods in Sections 3.1–3.5. Nonetheless, they still follow the generic principles of liquid patterning or shaping introduced in Section 1.

3.6.1. Molding

Molding—forcing LM into the topography of a pre-patterned substrate—is distinguished from stamping by the removal of the mold to create self-supporting metallic structures. LM composites (Section 3.5) or intermetallics with sufficiently large storage modulus, yield stress, and/ or viscosity can retain their shape even after removal of the mold.[130,135] Freezing LM can also help preserve the molded structure upon removing the mold.[146] However, gallium can undercool well below its melting temperature[17,21] (Section 2). Introducing a solid gallium seed into liquid gallium facilitates the nucleation process and enables the metal casting to solidify without much undercooling (**Figure 8**a).

In addition to challenges associated with preserving the molded structure, issues can arise while pressing the mold into a puddle of LM. Due to the low viscosity and high effective interfacial tension of LM, the LM will follow the path of least resistance, which unfortunately is often not into the small cavities of the mold; the use of thin film of LM helps.

3.6.2. Co-extrusion/Drawing of LM–Polymer Core–Shell Filaments

For practical reasons, it is often desirable for the LM pattern to be completely contained or encapsulated to avoid leakage or smearing of the LM features. This usually implies multistep fabrication procedures (see Sections 3.1–3.5). An alternative approach is to co-print LM with a polymer sheath,[147] which eliminates the need for the additional encapsulation or soft lithography step. The high surface tension and low viscosity makes it particularly difficult to produce continuous jets of LM as the liquid is prone to break up into streams of droplets (Rayleigh-Plateau instability).[1,2] However, when the LM stream is surrounded by a stream of higher viscosity fluid instead of air, increased viscous drag between the two phases can encourage "jetting"; that is, the formation of a continuous filament. With the appropriate combination of dispensing speeds, polymer viscosity, and nozzle diameters, continuous filaments of EGaIn coated in an elastomeric sheath can be extruded coaxially (Figure 8b).[147] The resulting fibers have LM core diameters in the 100 μm range.[150] Alternatively, it is possible to create wires of LM without an encasing layer using electrochemical oxidation to lower the interfacial tension so that the metal exits a nozzle as a cylinder.[151] The wires can be manipulated using a magnet to generate a Lorentz force that can temporarily suspend the wires against gravity.[152]

LM–polymer fibers can also be fabricated by "drawing", where an enclosed polymer pouch or tube containing LM is subjected to tensile stress to produce thinner and longer filaments. Drawing is used commercially to create optical fibers, but more recently has been used to create multifunctional fibers.[72,153] Depending on the type of polymer, the fiber may need to be drawn at elevated temperatures, or require subsequent curing, and would result in different mechanical properties. The two techniques described in this sub-section present the prospect of scalable fabrication of LM core–shell fibers, either in conjunction or separately, as they have the potential for automation. Regardless of how they are fabricated, LM–polymer core–shell fibers are highly versatile as they can be coiled,[147] entwined,[154] and even integrated into functional fabrics,[73,155,156] thereby confining LM within interesting shapes. A challenge for fiber-based conductors is identifying the best methods to make electrical connections externally and to other components.

3.6.3. Reactive Wetting of LM on Metallic Patterns

Large area LM thin films may be desirable for various applications, such as soft electrodes or mirrors. However, it is difficult to make smooth, large area, thin LM films on most substrates. Reactive wetting of LM on other metallic surfaces can be utilized to create smooth, thin LM films.[148,157–159] For example, LM can be spin-coated onto a Cu-coated substrate with HCl (Figure 8c).[148] During the spin-coating, the native oxides of LM and Cu are removed by HCl. Consequently, the LM can come into direct contact with the Cu surface, which allows it to reatively wet the Cu. Unlike regular selective wetting/ adhesion discussed in Section 3.4, reactive

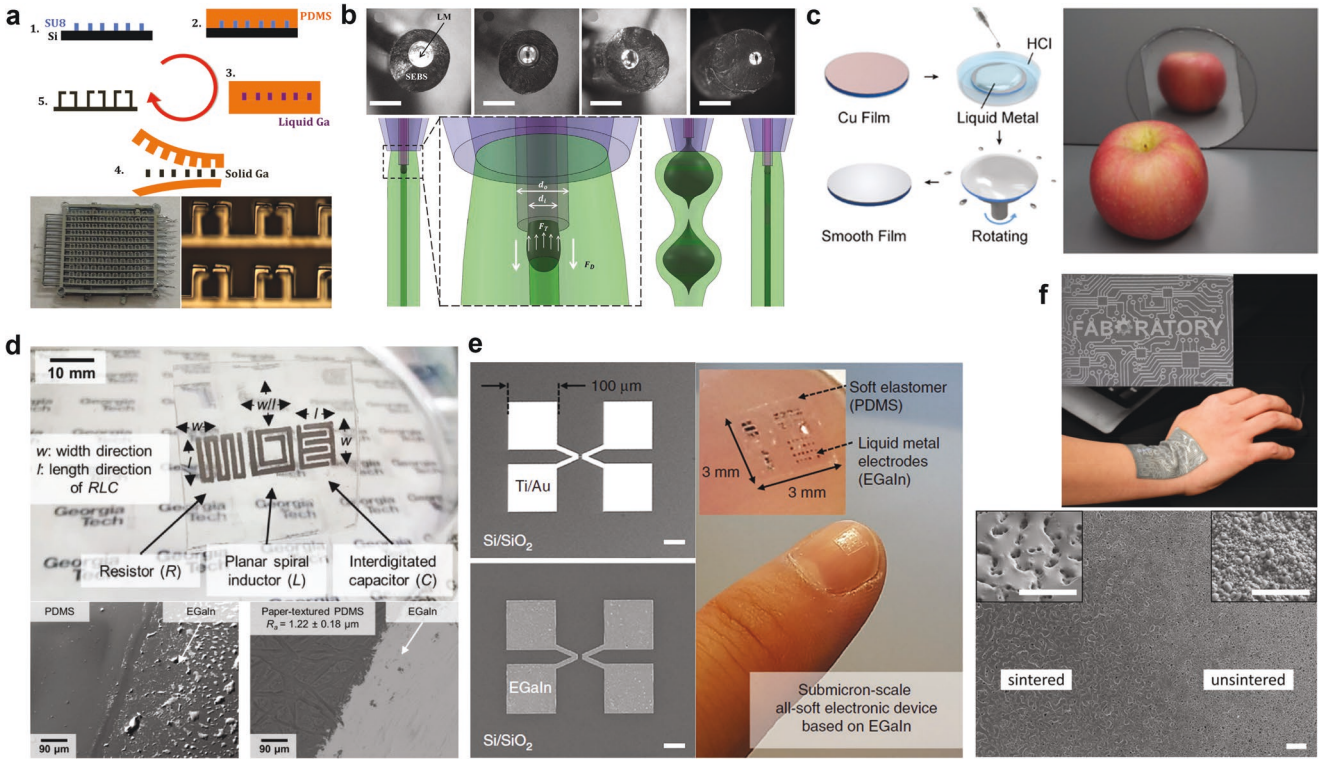

Figure 8. Other patterning approaches. a) Casting liquid Ga in a PDMS mold, followed by solidification of the metal prior to removing the mold.[146] b) Co-extrusion of LM–polymer core–shell filaments.[147] The presence of a viscous stream of polymer melt around the LM increases the viscous drag between the two fluids, thereby promoting jetting of LM. c) Thin LM film made by reactive wetting on Cu film (in the absence of native oxides).[148] d) LM pattern deposited on paper-textured PDMS by stamping. The quality of the stamped LM pattern is better on PDMS coated with cellulose microfibers compared to untreated PDMS due to better adhesion.[117] e) Ultra high resolution LM patterns made by a combination of imprinting and reactive wetting of LM to Au patterns.[119] f) Forming electrically conductive pathways by laser sintering LM nanoparticles.[149] Top: Difference in morphology between sintered and unsintered LM nanoparticles. Bottom: Laser sintering can be used to draw conductive circuits lines in an otherwise insulating film of LM nanoparticles on a flexible substrate. a) Reproduced with permission.[146] Copyright 2014, Wiley-VCH. b) Reproduced with permission.[147] Copyright 2019, Wiley-VCH. c) Reproduced with permission.[148] Copyright 2021, American Chemical Society. d) Reproduced with permission.[117] Copyright 2018, Wiley-VCH. e) Reproduced with permission.[119] Copyright 2020, Springer Nature. f) Reproduced with permission.[149] Copyright 2018, American Chemical Society.

wetting forms metal–metal bonds between the solid metal and LM, often resulting in the formation of a new phase along the interface. Such LM interactions with solid metals are complex and can even be destructive to the solid metal, as reviewed recently.[160]

Apart from to making large area LM thin films, the reactive wetting approach can also be used to fabricate more complex LM patterns, similar to what has been discussed in Section 3.4. Specifically, the initial solid metallic layer (Au/Cu) can be patterned using lithography processes. Then, LM (stripped of its surface oxide) will selectively remain within the areas of the metallic traces due to reactive wetting.[159,161]

3.6.4. Stamping

LM patterns can also be transferred to surfaces by applying LM onto the topographical features of a stamp and then pressing the stamp onto the substrate. For this kind of stamping (also called "additive stamping"), the transferred pattern follows the shape of the protrusions on the stamp (not the recesses). The stamps for transfer printing can be fabricated in a variety of ways, including soft lithography techniques.[117] Typically, the surface of the stamp is chemically modified so that it can carry LM. Likewise, the substrate onto which the LM pattern is meant to be deposited should have good surface adhesion with the LM native oxide. The lateral resolution of LM stamping can range from mm to cm scale and depends on how well the LM wets/adheres onto the substrate.[117] The pattern resolution on PDMS improved when it was surface-treated with cellulose fibers that enhanced the adhesion and pattern transfer (Figure 8d).[117]

3.6.5. Imprinting

Imprinting is similar to molding, except the LM remains within the mold. One of the first reports of imprinting[162] demonstrates the possibility of closely spaced, narrow LM lines as thin as 1 μm. Imprinting has been referred to as "reverse stamping" because it also involves pressing a mold into a body of LM, yet, the intention is to fill the recessed portions of the

mold.[117] Unlike stamping, imprinting is not a type of transfer printing process. One downside of imprinting (or molding) is the tendency of LM to flow along the "path of least resistance" during imprinting or to adhere to non-recessed portions of the mold; thus, it is not commonly utilized. To force LM into finer features, researchers have pressed the elastomeric molds onto "donor" substrates featuring very thin films of the LM, thereby making it harder for LM to flow away from the recesses.[117,119,162]

Lift-off Enhanced Imprinting: Lift-off uses a sacrificial layer to remove metal that adheres to non-desired parts of the surface. It can be used to improve imprinting; enhancing the wettability of the recesses in the mold makes them easier to fill with LM. The highest resolution features (lines as narrow as 180 nm width) were enabled by a combination of imprinting and reactive wetting (Figure 8e).[119] After using electron-beam lithography to prepare a topological PMMA mold with recesses coated with Au/Ti, the mold was pressed onto a flat LM film. Then the PMMA layer was lifted off to remove the excess LM, leaving only the targeted LM on Au/Ti within the originally recessed regions. This approach requires multiple steps but produces some of the finest features reported to date by harnessing the high-resolution capabilities of commercial lithographic techniques.

3.6.6. LM Particle Sintering Techniques

Films of LM particles typically do not form conductive, percolated paths. One common technique for achieving electrical percolation is called "mechanical sintering", which ruptures the oxide skin in response to an applied mechanical force.[163] This force can arise from simple pressing,[164] stretching,[145,165] or peeling[166] of elastomeric films containing LM particles. Mechanical sintering techniques, such as local pressing and peeling, have been successfully used to sinter liquid metal elastomer (LME) inks for direct write printing.[134] The oxide skin can also be ruptured to create conductive pathways by thermal and laser sintering (Figure 8f).[51,149] Though the concept of "selective laser sintering" is not new, the first application[149] of laser sintering to sonicated LM particles is a fairly recent development. Laser sintering is a highly effective technique when precise and selective conductive patterns are desired.[167] Moreover, "self-sintering" methods have been reported, where the drying of the water-containing solution results in a capillary force between adjacent particles that is sufficient to make them coalesce.[168] Freezing (at −80 °C) has also been shown as an effective sintering method for LM–silicone inks.[169] Termed as reversible transitional insulator and conductor (TIC), LM–polymer composites have also been reversibly sintered by tuning the temperature of the composite. When frozen, the metal expands to become conductive and recovers to an insulating state after warming.[170] More recently, it has been proposed that hydrogen doping of the oxide skin can enhance electrical conductivity between the LM particles without the need to rupture the oxide, thereby enabling printing of stretchable, conductive structures.[171]

3.7. Summary and Comparison of Patterning Techniques

Table 1 summarizes the major patterning techniques presented in this section by highlighting some of the key aspects of each approach. The information quoted in this table is to the best of our knowledge at the time of writing. The resolution values should be considered as an order of magnitude estimate and not a physical lower bound. It is our hope that future developments may broaden the results that can be achieved with a given patterning technique.

A prevalent theme in Table 1 is the tradeoff between ease of fabrication and resolution. Typically, to produce smaller LM features with better precision, more expensive equipment and steps are required. For example, stamping is probably the simplest and cheapest method since the stamp just needs to be made once, can be reused multiple times, and the process does not involve any special skills. The downside is that simple stamping has the poorest resolution out of the techniques discussed in this review and it can be messy. For improved pattern transfer, and thus, finer resolution, a more sophisticated method of stamping, which involves reactive wetting and lift-off could be employed. Though this lowers the smallest achievable feature size by 4–5 orders of magnitude, this process is more time consuming, has many steps, requires specific equipment and skills.

For practical uses, encapsulation of the LM is necessary to: 1) protect the fluidic conductive pattern from damage, 2) create elastic mechanical properties, and/or 3) prevent unwanted contact between LM and the user or other objects. Techniques such as injection/ vacuum filling and co-extrusion/ drawing of LM core filaments are advantageous in this regard since the containment of the LM is already an integral part of the patterning process. Yet these filling-based approaches require inlet ports and thus are poorly suited for creating many small, isolated metal features, like those used in circuits. Likewise, filaments are effectively 1D structures and therefore they cannot be used for applications that need more complex geometries. Microchannels also require fabrication steps and often plasma bonding of elastomers.[173]

To address the limitations of injection-based methods, other techniques described in the review first pattern the metal on a surface and then use additional encapsulation steps after patterning. This is rather straightforward for relatively flat designs, but can be quite tedious when it comes to LM patterns on curved surfaces (such as in Figure 5d[100]) and 3D structures (such as in Figure 7b[129]), especially when conformal coverage and uniform thickness of the coating are desired. A simplistic approach would be to cure the out-of-plane LM pattern in a block of elastomer or resin, but that would add bulk to the part. It is possible to spray coat silicone elastomers, which offers a way of making a thin, conformal encapsulation.[99]

Often, the high surface tension of LM is regarded as problematic since it hinders processes like filling, coating, and mixing. Methods like injection filling, stenciling, and direct writing would be easier for fluids with lower surface tension. Yet, certain processes capitalize on the high surface tension of LM to achieve desirable outcomes. For example, the high surface tension of LM enables good selectivity in selective adhesion and reactive wetting, resulting in well-defined patterns.

Table 1. Summary of liquid metal (LM) patterning techniques.

Patterning technique	Patterning enabler	Special condition(s)	Typical substrates/ matrices	Lateral feature size (order of magnitude)	Electrical behavior	Resulting structure
Injection filling	Embedded channels, hollow capillaries (inlet and outlet ports necessary)	Pressure applied to LM to overcome interfacial forces	Elastomers, plastics, 3D printed parts, hollow fibers	5 μm–mm[60,66,67] 150 nm (using large pressures and rigid capillaries)[172]	Metallic conductivity	LM features contained in channels
Vacuum filling	Embedded channels (outlet ports not necessary)	External vacuum followed by restoring atmospheric pressure	Elastomer, plastics, 3D printed parts	5–100 μm[68,69]	Metallic conductivity	LM features contained in channels
Shear-driven direct writing of LM	Nozzle, CAD drawing	Dispensing pressure and vacuum. Control over gap between nozzle & substrate	Smooth surfaces on which LM oxide can establish good adhesion[49]	2–100 μm[50,85] (size defined by nozzle diameter)	Metallic conductivity	LM patterns on planar substrates, conjoined LM drops, out of plane cylinders
Extrusion-based direct writing of LM-matrix paste	Nozzle, CAD drawing	Dispensing pressure	Various surfaces	μm–mm[129,131]	10^6 S m^{-1} conductivity[129,131]	Planar and 3D metallic structures
Extrusion-based direct writing of LM particle in polymer dispersion	Nozzle, CAD drawing	Dispensing pressure	Curable polymers (e.g., PDMS)	100 μm[134]	Electrically insulating to 10^{-2} S m^{-1} conductivity (after mechanical sintering)[134]	Planar and 3D LM–polymer composite structures
Co-extrusion of LM in polymer sheath	Multichannel nozzle	Dispensing pressure, elevated temperature, subsequent thermal drawing (optional)	Thermoplastic, thermosetting polymer	10–100 μm[147]	Metallic conductivity	Hollow polymer filaments with LM core
Laser sintering of LM particle dispersion	CAD drawing	Focused laser beam	Volatile carrier fluid (e.g., ethanol)	10–100 μm[51,149]	10^5–10^6 S m^{-1} conductivity (after laser sintering)[149]	Planar conductive patterns in a film of unsintered LM particles
Stenciling of LM	Stencil	Compressed gas (for spray deposition)	Surfaces on which LM oxide can establish good adhesion	>100 μm[99–101] 10 μm (with custom stencil)[98]	10^4 S m^{-1} conductivity (spray deposited)[100]	Planar LM patterns on substrates
Additive stamping of LM	Stamp	Importance of adhesion	Surfaces on which LM oxide can establish good adhesion	mm–cm[117]	Metallic conductivity	Planar LM patterns on substrates
Imprinting (reverse stamping) of LM	Stamp	Importance of adhesion	Surfaces on which LM oxide can establish good adhesion	μm–mm[117] 100 nm (lift-off enhanced)[119]	Metallic conductivity	Planar LM patterns on substrates or embedded in recesses
Selective adhesion of LM	Prepatterned substrate	Importance of adhesion	Surfaces with LM-phobic and LM-philic regions	100 μm[60,114]	Metallic conductivity	Planar LM patterns on substrates, LM features contained in channels
Reactive wetting of LM	Prepatterned solid metal traces	Acidic/ basic solution or vapor to remove native oxide(s)	Au, Cu, Cr adhesion layer	10 μm[148,157–159,161]	10^6 S m^{-1} conductivity[148]	Patterned LM thin film on solid metal adhesion layer (with some intermetallic in between)

4. Applications

The ability to control the shape of LM enables many applications that utilize the unique properties of LM. Applications of LM have been reviewed in several articles recently,[31,174–181] so we only briefly touch on some illustrative examples while highlighting some other interesting patterning approaches.

4.1. Stretchable Conductors

4.1.1. Stretchable Conductive Wires

Using LMs for stretchable and soft electronics has been widely explored in recent years.[184] LM can be direct printed into patterns followed by encapsulation with elastomeric materials to make stretchable conductive wires. For example, **Figure 9**a shows serpentine LM wires printed on a silicone substrate by direct writing. The wires were then spin-coated with silicone polymer to create stretchable wires (right side of Figure 9a). In addition to direct writing, LM can also be injected into a hollow elastomer fiber to make stretchable conductive fibers (Figure 9b).[66] These stretchable conductors typically only fail when the encasing polymer fails (e.g., > 1000% strain in many cases). At more modest strains (e.g., 100% strain), LM conductors have proven reliable for 10000+ stain cycles.

4.1.2. Interconnects

Similar to the fabrication of conductive fibers, LM can be injected into microchannels within elastomer slabs in 3D structures to create stretchable 3D interconnects (Figure 9c).[182] However, using injection to pattern stretchable LM-filled conductors relies heavily on the design of the elastic containers (e.g., tubes, channels), which can be time consuming to fabricate as they often require multistep, tedious fabrication procedures.

Alternatively, rheologically modified LM pastes can be extruded or molded to adopt 3D structures without external support due to their increased mechanical resistance to flow (Figure 9d).[131] For example, Figure 9e shows a stacked circuit with vertical interconnects fabricated by direct printing an EGaIn-Ni paste.[129] Encapsulating the 3D printed stacked circuit in elastomer results in a stretchable and conductive structure. Although incorporating solid additives (nickel particles) decreases the fluidity of the mixture, the encapsulated LM paste structure could sustain up to 300% tensile strain and ten stretch-relax cycles under 200% strain without losing electrical conductivity.

Evaporating LM onto solid metal traces is another strategy to achieve stretchable LM patterns. Specifically, gold can first be sputtered onto a silicone substrate through a shadow mask. The gold layer serves as a template for LM to adhere and bond to during LM evaporation via metal–metal bonding to form a biphasic layer. The excess metal is removed during the lift-off step, leaving the desired metallic pattern (Figure 9f).[183] This results in a thinner trace (<1 μm in thickness) relative to that of direct writing and is appealing because it is compatible with lithography. The resulting biphasic layers can be assembled to create a multilayered interconnect, as shown in Figure 9g. Note that, care should be taken when thermally evaporating gallium because of its tendency to embrittle certain metals, which might damage expensive deposition equipment.

4.2. Soft Sensors

A recurring theme among the numerous papers reporting LM-based sensors is that geometric changes to the LM during deformation cause measurable changes to certain electrical properties (**Figure 10**a). Examples include strain-dependent (or stress-sensitive) resistance,[188] capacitance,[154] inductance,[189] or induced potential/current[190] realized through a myriad of configurations. Techniques for patterning LM are very relevant to making soft, LM-based sensors as they determine what configurations and structures are possible and what the starting geometry-specific properties of the device could be.

4.2.1. Injection Filling

LM-filled elastomeric fibers can serve as capacitive sensors of different kinds of deformation and touch.[154] Such fibers can detect changes in capacitance arising from the presence of a human finger and therefore are tactile sensors. A pair of such hollow fibers injected with LM (cf. Figure 8b), when entwined (Figure 10b), exhibited increasing capacitance between the fibers with increasing applied torsion. The fiber double helix could also sense tensile strain capacitively as tension increased the contact area, and thus capacitance, between the two fibers. Injection filling is a popular approach to create LM-based sensors. In the sensor designs presented in these papers[154,188–194] the LM parts were fully embedded in elastomer for protective encapsulation (to avoid leakage) and to ensure predictable elastic deformation that gives rise to geometric changes to the LM for sensing.

4.2.2. Direct Writing

Though not as straightforward as injection filling, direct writing has been shown to be a viable method for depositing conductive LM patterns on flexible substrates for sensing applications. Thus far, printing of all three types of LM-based inks—namely: i) LM,[185] ii) LM pastes,[195] and iii) LM droplet suspensions[171]—have been employed in fabrication processes of sensor parts. Figure 10c shows a glove with multimodal sensing and feedback capabilities created by direct writing.[185]

Figure 10d shows an example of a printed coil composed of LM droplets in elastomer.[171] When deformed, the device changes its geometry and therefore its inductance, which can be correlated to strain.

4.2.3. Stenciling and Molding

LM can be shaped into functional sensing components through a combination of patterning strategies, not just one.

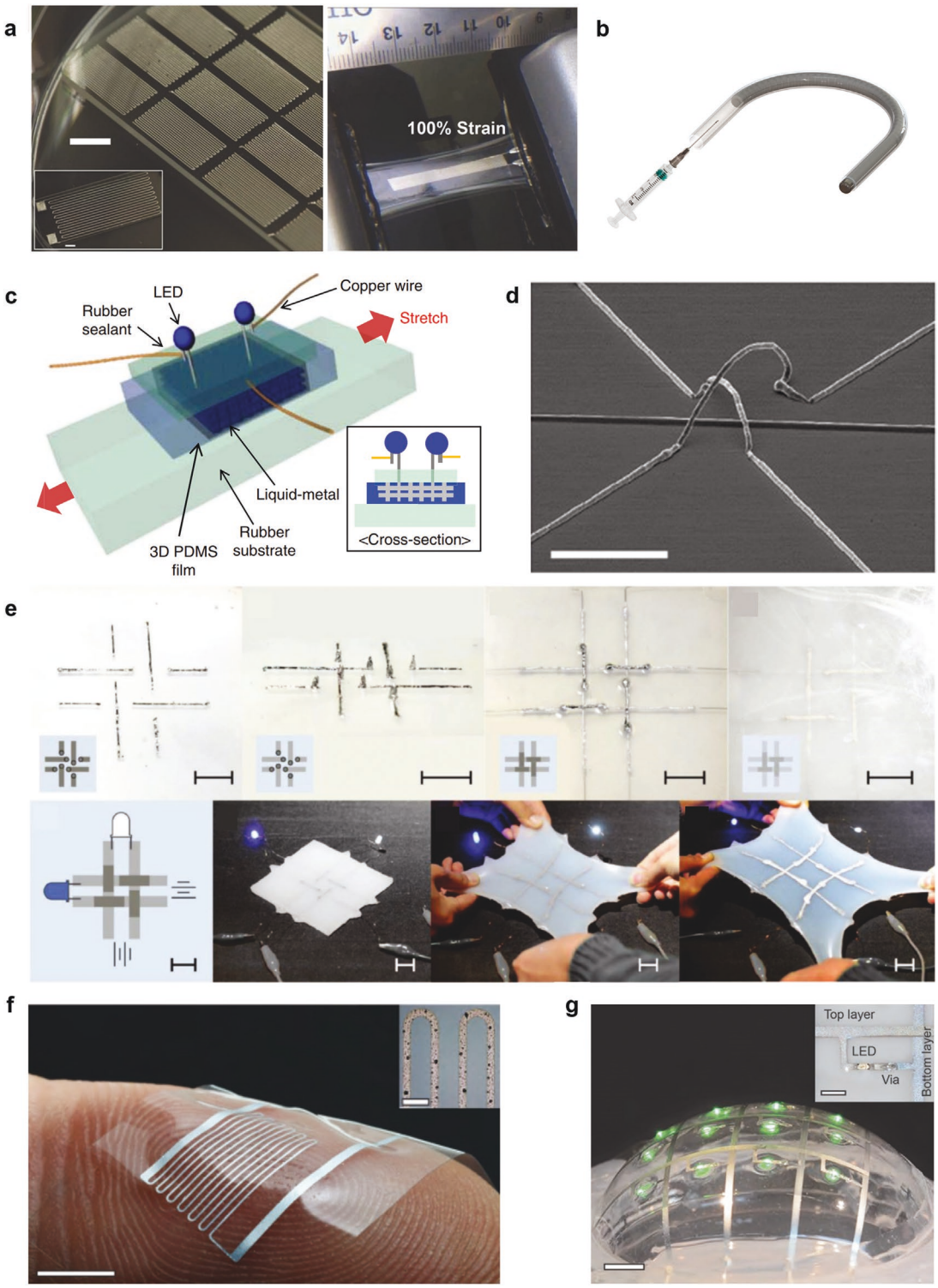

Figure 9. Stretchable and soft conductors consisting of patterned LM encased in or on elastomers. a,b) Stretchable LM wires made by direct writing (a)[92] and injecting LM into an elastic capillaries (b). c) Stretchable conductors made by filling LM into pores in a silicone slab.[182] d) Self-supporting and spanning LM interconnects fabricated by extrusion of CNT–LM composite.[131] e) Multilayer stretchable circuit with vertical interconnects fabricated by direct printing an EGaIn-Ni paste followed by encapsulation in elastomer.[129] f) Biphasic Ga/Ga-Au thin film deposited on PDMS.[183] g) Multilayer stretchable interconnects fabricated by thermal evaporation through a stencil coupled with reactive wetting.[183] a) Reproduced with permission.[92] Copyright 2014, Wiley-VCH. c) Reproduced with permission.[182] Copyright 2012, Springer Nature. d) Reproduced with permission.[131] Copyright 2019, American Chemical Society. e) Reproduced with permission.[129] Copyright 2018, Wiley-VCH. f,g) Reproduced with permission.[183] Copyright 2016, Wiley-VCH.

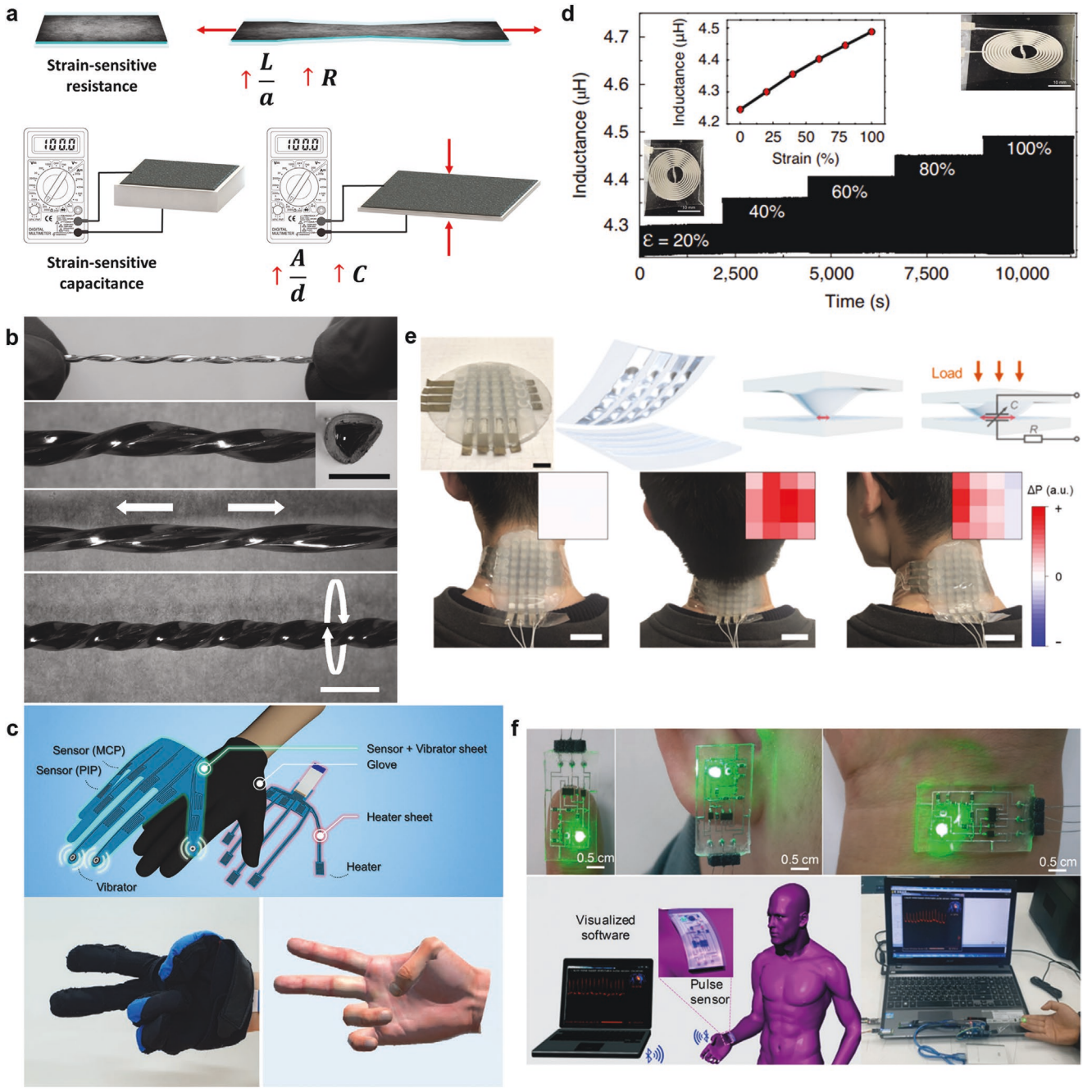

Figure 10. Stretchable sensors made of patterned LM encased in elastomer. a) Geometric changes (i.e., area, *A*, length, *L*, thickness, *d*) during deformation can be used to sense strain or stress via changes to resistance, *R*, or capacitance, *C*, for example. b) Twisted LM-filled elastomer fibers as capacitive sensors of touch, strain, and torsion.[154] c) A glove that can sense motion and provide vibrational and thermal feedback using LM patterned by direct writing.[185] d) Inductive sensor patterned by direct writing of H-doped LM particle suspension.[171] e) Capacitive pressure sensor consisting of an electrode shaped as an array of "icicle" geometries patterned by stenciling and molding.[186] f) Wireless pulse sensor containing stretchable LM interconnects patterned by reactive wetting.[187] b) Reproduced with permission.[154] Copyright 2017, Wiley-VCH. c) Reproduced with permission.[185] Copyright 2021, Wiley-VCH. d) Reproduced with permission.[171] Copyright 2021, Springer Nature. e) Reproduced with permission.[186] Copyright 2020, American Chemical Society. f) Reproduced with permission.[187] Copyright 2017, Royal Society of Chemistry

For example, LM "icicles" were created by stenciling followed by molding (Figure 10e).[186] First, strips of LM were patterned using a stencil and then secured in place with an elastomer topcoat. Then, the multilayered composite was placed on a grid in a vacuum chamber. As the vacuum was being vented, the pressure gradient from the influx of air to the chamber caused the composite to get pressed against the grid, which left icicle-shaped protrusions and impressions on its soft surface. To secure the array of crests and valleys from the grid impression, another layer of elastomer was cured over the back of the

composite. This approach is noteworthy as it produces out-of-plane features from an initially flat sheet in two efficient steps and the resulting structure was elastic and stable. The array of silicone-encapsulated LM "icicles" constituted an electrode in a capacitive touch (pressure) sensor; paired with a flat LM electrode, the capacitance between the two LM electrodes increased with increasing compressive pressure flattening the LM "icicles" against the flat electrode.

4.2.4. Reactive Wetting

Reactive wetting has been used to create stretchable interconnects to circuits designed for sensing. For example, LM can wet Cu patterns on PDMS in the absence of the oxide.[187,196] Figure 10f shows a soft sensor of heartbeat (pulse) using LM circuits. The LM patterns were deposited by reactive wetting on Cu-plated Au lines and served as stretchable interconnects providing electromechanical interfacing between the rigid electronic components and the soft, elastic substrate. The resulting device could conform to the irregular contours of the human body, sense the wearer's pulse, and transmit the data wirelessly. Furthermore, the device was able to function even as the wearer engaged in physical exercise. This demonstrates the utility of this LM patterning technique in fabricating practical sensing devices in which not all the components can be substituted with soft materials.

4.3. Self-Healing and Reconfigurable Conductors

The fluidity of LM distinguishes it from solid metal in useful ways. LM flows readily in response to applied stress without losing its inherently high conductivity. This feature is the basis for the mechanism of self-healing and reconfigurable LM-based electronic devices.

4.3.1. Healable

Figure 11a shows an elastomer containing LM particles. The particles are mechanically sintered into a patterned circuit using a pen plotter. The circuit is evident from the dark regions on the

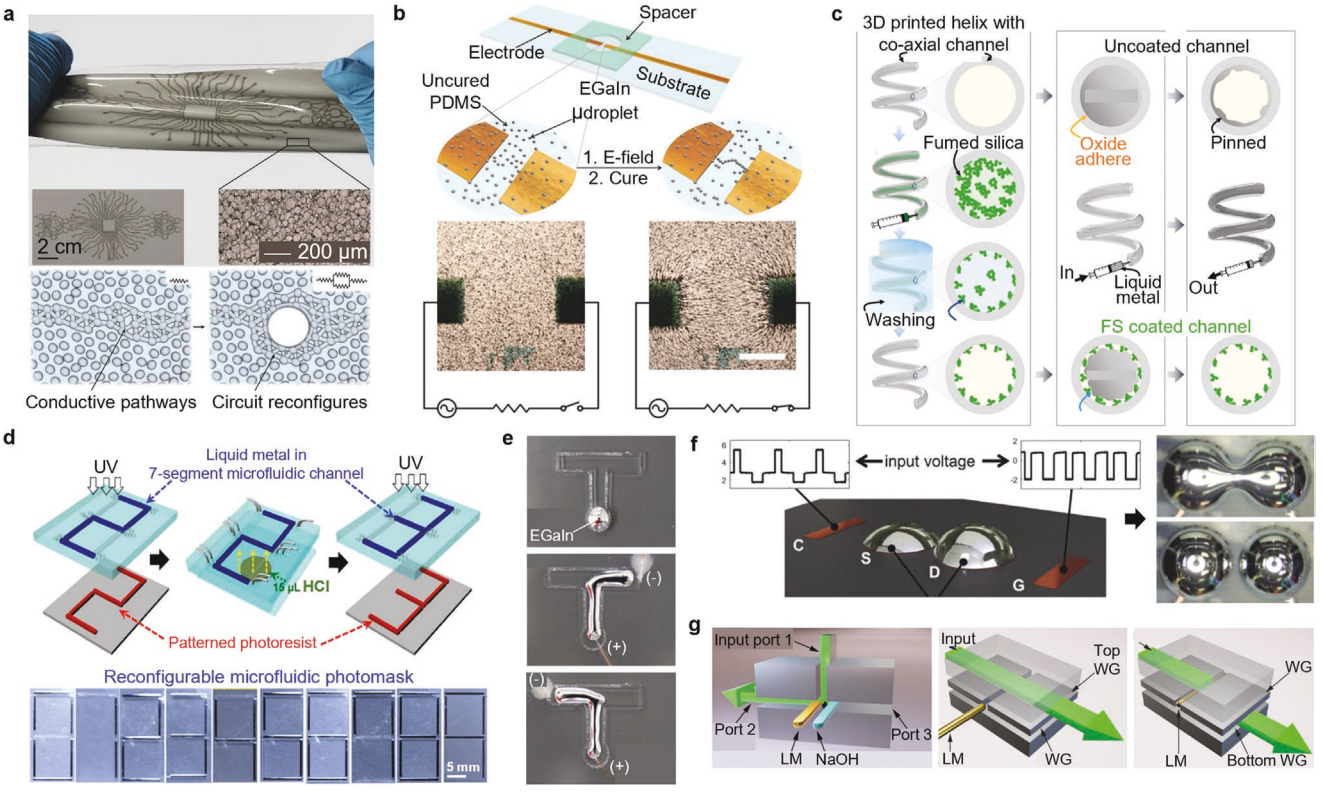

Figure 11. Self-healing and reconfigurable LM-based electronics. a) Electrically self-healing LM-elastomer conductor. Mechanical stress from cutting causes LM particles surrounding the damaged area to rupture and coalesce, effectively "re-routing" the conductive pathways.[53] b) Electrically and mechanically healable stretchable conductors assembled by dielectrophoretic motion of LM droplets in uncured elastomer.[197] c) Surface-treated "metallophobic" channels for reconfigurable LM-based circuitry inside 3D printed parts.[60] d) Reconfigurable LM-filled microfluidic photomask in which the LM shapes block light from reaching an underlying photoresist.[198] e) Interfacial tension modulation via electrochemical oxidation of LM in NaOH solution to direct the flow and shape of LM in a channel.[199] f) Programmable coalescence and separation of two anchored LM droplets in a fluidic switch.[200] g) Actuation of LM slugs by continuous electrowetting to steer terahertz electromagnetic radiation through different pathways.[83] a) Reproduced with permission.[53] Copyright 2018, Springer Nature. b) Reproduced with permission.[197] Copyright 2020, Wiley-VCH. c) Reproduced with permission.[60] Copyright 2020, American Chemical Society. d) Reproduced with permission.[198] Copyright 2014, IEEE. e) Reproduced with permission.[199] Copyright 2014, National Academy of Sciences USA. f) Reproduced with permission.[200] Copyright 2017, Wiley-VCH. g) Reproduced with permission.[83] Copyright 2018, Springer Nature.

sample. When cut, a small amount of LM shears onto the surface of the cut from the exposed LM particles, creating new conductive pathways along the rim of the cut, effectively "re-routing" the conductive pathways.[53] This composite heals autonomously (without external intervention). This concept was used to demonstrate a self-repairing circuit and a soft robot which could continue functioning even after significant damage.

Field-Driven Assembly for Healing: Through a process called dielectrophoresis, LM microdroplets suspended in silicone pre-polymer could be directed, and therefore patterned, by applied electric field to assemble into conductive traces (Figure 11b).[197] These assembled particles form conductive paths that can make connections between electrodes. After assembly, the silicone pre-polymer can be cured to preserve the shape and create stretchable conductors. Thus, this approach can also be used to repair or rewire portions of circuits.

4.3.2. Reconfigurable

Pressure-Induced Flow: An intuitive approach to making liquid patterns reconfigurable is by applying pressure to pump the fluid into or out of channels. However, the surface oxide readily adheres to most surfaces such that it is difficult to completely remove LM without leaving behind some pinned oxide and LM residue. One way around this is to reduce the adhesion between the oxide and substrate via surface roughness so that oxide pinning can be averted. For example, coating plastic surfaces with silica particles makes them nanoscopically rough (10–100 nm scale), effectively rendering them "metallophobic."[60] This solution-based coating method could also coat the interior surfaces of 3D printed channels (Figure 11c). LM could be injected and withdrawn from surface-treated channels repeatedly to make variable area capacitors.

Another way to enable smooth flow and clean detachment of LM within channels to create reconfigurable patterns is by chemically removing the oxide skin using an acid or base. This principle has been used to make a reconfigurable microfluidic LM photomask (Figure 11d).[198] Injecting LM into a PDMS microfluidic channel creates light-opaque and light-transparent regions of the desired pattern. To demonstrate this concept, LM could be shaped into digits from "0" to "9" on the same PDMS microchannel, and the patterns transferred clearly onto the underlying photoresist upon UV exposure.

Apart from mechanically reconfiguring the shape of LM, another approach is to exploit the dramatic and reversible changes in interfacial tension that can be achieved electrochemically.[151,199,201] Applying oxidative/ reductive potential to a puddle of LM immersed in an electrolyte results in reversible formation/removal of surface oxide species. This modulates interfacial tension of LM in NaOH solution substantially from ≈500 mJ m^{-2} (bare metal in electrolyte) to near zero by applying small electric potential (Figure 11e).[199] This principle can reversibly shape and direct the flow of LM in capillary and planar channels by modulating the interfacial tension. This electrochemically-induced reconfigurability of LM can be extended to interesting applications such as fluidic switches and microactuators. In one example, LM was patterned by wetting two hemispheres onto solid Cu pads. By electrochemically modulating the interfacial tension of two anchored EGaIn droplets in NaOH solution, the droplets could be programmed to coalesce ("on", conductive) or separate ("off", insulating) on demand, (Figure 11f).[200]

Continuous Electrowetting: Continuous electrowetting enables electrically-controlled flow of LM slugs or droplets in an electrolyte. An electrical double layer forms at the interface of LM in electrolyte. Applying an electric field to the solution alters the distribution of charges in the electrical double layer which manifests as local interfacial tension gradients that propel the LM droplet in a direction. Continuous electrowetting can enable reconfigurable terahertz (THz) devices (Figure 11g).[83] The devices consist of capillaries filled with a slug of LM in aqueous NaOH. While aqueous NaOH has a large absorption coefficient throughout the THz range, LM is reflective. By applying DC voltage across the electrolyte, the LM plug can be made to move through the capillary, in and out of the output port of the waveguide, offering excellent isolation and switching performance.

4.4. Energy Harvesters

This section briefly discusses the use of LM in energy harvesting. A detailed review of LM-based energy harvesting mechanisms is out of the scope of this work, however comprehensive reviews on soft, LM-based energy harvesting have been recently published.[180,181]

4.4.1. Mechanical Energy Harvesting

Triboelectric Generators and Piezoelectric Generators: In the literature the term Triboelectric generators (TENG), also known at times as TEG, is used in reference to triboelectric nanogenerators even though "nano" has no real physical significance. Here the abbreviation TENG will be used instead of TEG not to confuse it with thermoelectric generators and to be consistent with the literature. TENG devices rely on materials that can become statically charged when rubbed against one another (e.g., a balloon rubbed against hair).[206] Moving such charged surfaces toward and away from each other can induce the flow of charge to and from sub-surface electrodes. This simple and low-cost approach converts mechanical to electrical energy. An excellent comprehensive review explains the history, physics, controversies, and evolution of triboelectric charging.[207]

LMs provide excellent mechanical compliance and electrical conductivity that can enable new modes of deformation and new applications of TENGs. For example, TENG using LM as an electrode material and silicone rubber as the triboelectric layer resulted in power density of 8.43 mW m^{-2} (**Figure 12**a).[202] The LM was injected into a molded silicone cavity. Another study improved the mechanical compliance and long-term durability by incorporating LM inclusions into high-dielectric polymers, reaching 13.95 mW m^{-2}.[208] In a more recent study, an elastomeric composite composed of large EGaIn droplets in Ecoflex capitalized on the sedimentation of the denser droplets to form phase-separated conducting and insulating regions. The LM-elastomer composite was shaped using a stencil before the mixture cured. From a patterning standpoint, this fabrication

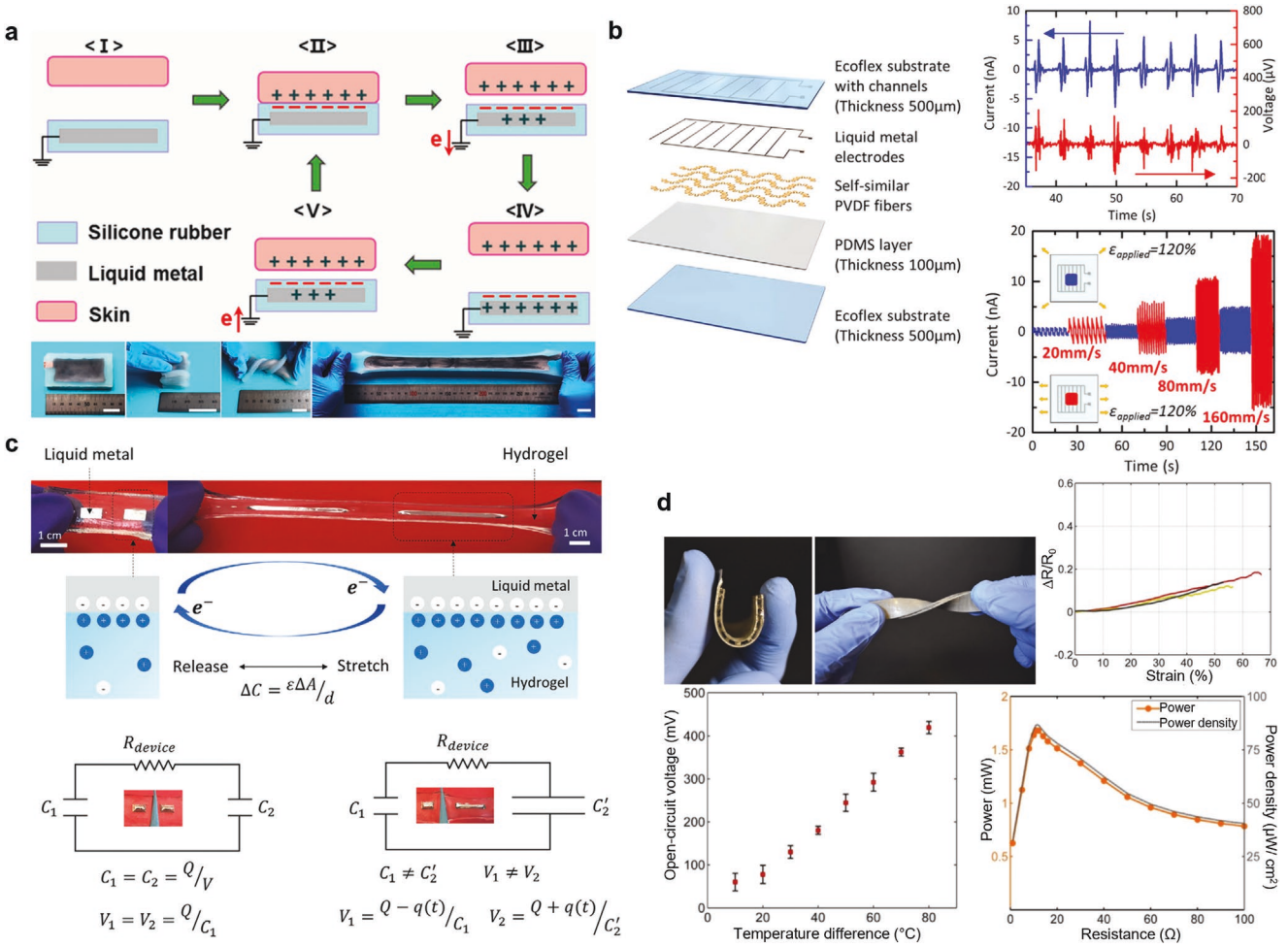

Figure 12. Energy harvesters using patterned LM. a) LM-based triboelectric generator using LM as an electrode material and silicone rubber as the triboelectric layer.[202] b) Interdigitated microfluidic EGaIn electrodes made by injection within a piezoelectric energy harvester.[203] c) Variable area, electrical double layer capacitor consisting of LM electrodes encapsulated in hydrogel for mechanical energy harvesting.[204] d) LM-elastomer composite as interconnects for a thermoelectric generator.[205] a) Reproduced with permission.[202] Copyright 2018, American Chemical Society. b) Reproduced with permission.[203] Copyright 2017, Elsevier. c) Reproduced with permission.[204] Copyright 2021, Wiley-VCH. d) Reproduced with permission.[205] Copyright 2020, American Chemical Society.

method is unique because it only requires one mixture and a single deposition step to produce two distinct regions that will not delaminate. The flexible TENG using this configuration exhibited high stretchability (above 500% strain), mechanical stability (over 10 000 cycles), and a max peak power of 1 mW cm^{-2}, which is sufficient to power a hydro-thermometer with a digital display.[209] TENGs can also be made by simply injecting LM into stretchable, hollow fibers.[156]

LM electrodes have been used in a highly stretchable triboelectric nanogenerator enhanced using a composite of piezoelectric particles dispersed in elastomer.[210] The device produces a V_{oc} of 1.38 kV, an I_{sc} of 36.12 μA, and power density of 1.1 mW cm^{-2}. Another study contacted piezoelectric PVDF microfibers with LM injected into silicone microchannels (Figure 12b).[203]

Electrostatic Energy Harvesters/Variable Area Capacitors: Electrostatic energy harvesters can harness mechanical energy by changing the area or dielectric properties of a capacitor. By increasing and decreasing the capacitance, charge can be pumped in and out of the capacitor through an external circuit. This concept has been demonstrated to harvest energy through shape deformation or injection of liquid slugs placed between two electrodes or encased in a soft elastomer.[211,212]

When a conductor interfaces with an electrolyte, it forms an electrical-double-layer capacitor (EDLC). One attribute of EDLC is the small distance that separates opposite charges, resulting in high capacitance (on the order of 10 s of mF m^{-2}). While there are several approaches to creating stretchable EDLCs, they do not vary the interfacial area between the conductor and the electrolyte when deformed.

LM electrodes can deform and therefore change their area. Thus, it is possible to create an all-soft variable area capacitor for energy harvesting composed of LM electrodes interfacing electrolyte within a hydrogel (Figure 12c).[204] Molded rectangles of LM encased in hydrogel change area in response to stretching, pressing, or twisting, thereby changing the EDL and capacitance. The ultra-stretchable device (>400% strain) was able to generate a power density of 0.5 mW m^{-2} under 25% strain.

4.4.2. Thermoelectric Generators

Thermoelectric generators (TEGs) harvest thermal energy and convert it directly to electricity. This can be useful for harvesting thermal energy from the body but doing so requires a soft device that can conform comfortably to the skin and work efficiently given the small difference in temperature between the body and environment.

Typical TEG structure consists of small pieces of p and n type semiconductors connected electrically in series between two regions of different temperatures, a hot side and a cold side.[213] These semiconductors are normally connected by rigid metal interconnects. By connecting them with LM, it is possible to create soft and stretchable TEGs. This approach is interesting because it enables the use of semiconductors with best-in-class Seebeck coefficients (S), which characterize how a material converts a thermal gradient to potential difference.[214]

LM is an effective option for metal interconnects in TEGs.[215] In one study, LM interconnects resulted in extremely low resistance and impressive flexibility. The LM interconnects were patterned through a combination of selective wetting and stenciling to produce mechanically robust TEGs.[216] In another study, LM deposited by spraying through a stencil on Ecoflex produced a soft TEG (termed STEG by the authors) that produced 19.8–40.6 $\mu W\ cm^{-2}$ under a $\Delta T = 20$ °C and can withstand over 20% strain.[215] LM particles can be mixed into the elastomer to improve the thermal conductivity, which further improves performance.[217]

LM elastomer composites (LMEE) have been used as stretchable thermal interfaces for favorable heat transfer. Their mechanical compliance enables conformal contact on dynamic surfaces with curvature, such as human skin, which facilitates heat flow from the human body and maintains the temperature gradient necessary for efficient energy generation.[205] The ability of LM to supercool (as low as −80 °C) in LMEEs allows them to be used in compliant state over a wide range of temperatures (Figure 12d).[18]

5. Challenges and Opportunities

This review highlights approaches to pattern LM that utilize the general principles highlighted in Figure 1. The ability to pattern LM is a useful and enabling tool. Going forward, the following challenges and opportunities may be considered.

5.1. Resolution

The resolution of LM structures depends on the patterning method and the demands of the application. For soft devices or metallized 3D printed parts, in which LMs find use as antennas, electrodes, and interconnects between larger components, a resolution of tens to hundreds of micrometers is usually sufficient. This can be accomplished using almost all the methods discussed in this review. Yet, the ability to make smaller structures below the detection limit of the eye (a few micrometers) can enable stretchable, transparent conductors.[218] Interconnects between dense transistors also require higher resolution features (micrometer scale). Smaller structures can also enable useful optical effects, such as nano-structures for plasmon resonance.[219,220] In addition to resolution, patterning requires consideration of "line edge roughness". For example, stencil printing is an easy way to pattern LMs, but it offers poor control over line edge roughness. Thus, there are often trade-offs with patterning: the easiest methods to implement for new users often have the poorest resolution and worst line edge roughness. Selective wetting is one of the most attractive approaches because it utilizes lithographic patterning to create conductive pathways and can produce high resolution features by harnessing (rather than fighting) interfacial forces. Yet the lithographic patterning of wetting surfaces requires an extra step that is not easy to implement on all substrates (including elastomers). Selective wetting also creates interfaces between LM and solid metal traces that may have poor long-term stability.

5.2. Interfacing

In many applications, such as electronics, the ability to pattern LMs is only useful if the metal can make conductive and stable contacts to other materials and components. Currently, LM electronic components and circuits are connected to external electronics using solid metal wires or thin films and physically secured with soft encapsulation (e.g., silicones). To establish low contact resistance at the LM-solid metal junction, the LM oxide skin has to be etched first to enable reactive wetting, such as in refs. [187,196]. Otherwise, depositing LM on solid metal in the absence of etchants could still produce electrically conducting contacts, like the LM-FFC (flat flex cable) interconnects in,[185] which are adequately robust as demonstrated by the device's ability to function even under flexure.

The ability of LM to wet other metals is a convenient route to making low-resistance contacts, yet its ability to embrittle and damage certain metals leads to poor stability.[160] In our laboratory prototypes, contacts with certain metals, such as Cu, appear to be sufficiently stable, but these contacts need to be studied more rigorously for long term stability. To date, thin, conductive coatings of carbonaceous materials (PEDOT, graphene) have been used to protect metal contacts from LM while maintaining conductivity.[221,222] Certain metals, such as W and Mo, have excellent stability when contacted to LM and might also serve as diffusion barriers. Alternatively, it is possible to use other approaches, such as aligning conductive particles vertically through the thickness of an otherwise insulating film (so-called Z-tape) to make stretchable contacts.[223] The role of the native oxide layer(s) on contact resistance also presents an opportunity for additional study.

5.3. Adhesion

Many patterning methods require or benefit from adhesion to a substrate. Conversely, the ability to move plugs of LM in channels requires poor adhesion. The adhesive behavior of LM at interfaces is often mediated by the native oxide, yet its interactions with substrates is poorly understood. The oxide layer adds a mechanical film to the surface of the metal and creates two new interfaces: LM/oxide and oxide/air. The oxide does not "wet" surfaces;

instead, it adheres. Conventional static contact angle measurements are either irrelevant or provide minimal insight due to the mechanical effects of the oxide on drop shape, yet such measurements permeate the literature despite advice otherwise.[40] The chemical composition, smoothness (wrinkles), and hysteresis of the handling of the oxide (i.e., whether it is under tension or not) may further affect adhesion. In addition, the adhesive behavior appears to depend on whether the metal is volumetrically advanced against a surface, versus simply contacting it.[41]

5.4. New Functionality and Applications

LM offers truly special properties. 1) Metallic conductivity (electrical and thermal) and optical properties. 2) Supercooling (wide temperature window as a liquid), low toxicity, and effectively zero vapor pressure at room temperature. 3) Expansion upon freezing. 4) The ability to mix other materials into the metal. 5) Unrivaled combination of conductivity and deformability. Can such unique properties be utilized for new applications?

5.5. Nozzle Dispensing

One of the distinguishing aspects of LM relative to other conductors is the ability to dispense it from a nozzle. Printing bulk LM requires excellent control over the distance between a nozzle and substrate.[96] To make it easier to print, several studies have modified the rheology of the LM. There are opportunities to build on this work to make LM easier to print in a consistent manner and therefore more broadly adapted to new users.

5.6. 3D Patterning

Conventional printed circuit boards and integrated circuits typically have multiple levels of metals to interconnect components. Perhaps such sophistication is not necessary for LM circuitry, but it nevertheless represents a patterning challenge.

5.7. Process Integration

To date, LMs have shown a lot of promise in academic labs and even find use as thermal materials for dissipating heat in electronics such as the Sony Playstation, but they have not been widely adopted as electrical conductors in commercial applications. What problems can LM solve? Can LM be adopted to existing processes? Can challenges associated with patterning and handling be addressed?

5.8. Scalability

In principle, every patterning technique discussed in this review can be automated to a greater degree, provided it is possible to use processing equipment built from materials—such as plastics—that can withstand prolonged contact with LM. Since there are few examples of commercial devices using liquid metals as electrical conductors, we can only speculate on some of the considerations and challenges involved with scaling since our own studies have been in the context of an academic laboratory.

A key consideration—beyond the ability to pattern metal into desired shapes and locations—is whether the LM must make contact with other electronic components and materials necessary to create circuits or devices. Typically, electronic componentry (e.g., chips, sensors, capacitors) are placed at desired locations by "pick and place" techniques. The LM can wet the metal contact pads on such components,[196] similar to existing manufacturing approaches that use solder. The longevity of such contacts deserves further study.

Microchannels can be mass produced by molding and subsequently filled with LM in a hands-free manner using vacuum filling. In principle, electronic components could be molded into the microchannels so that the filling creates interconnects within the channels, but this represents an additional step. Thus, filling-based approaches seem best suited for making simple conductors such as wires or antennas or for metallizing capillaries inside molded or 3D printed parts.

Exposed LM patterns can be deposited rapidly on substrates through a stencil or by stamping. These examples have the potential for manufacturing at scale since they share essential features with existing manufacturing techniques (e.g., screen/stencil printing of t-shirts or roll-to-roll printing of print media). Yet, one unique consideration of LM "ink" is the possibility of the accumulation of surface oxide that may result from reusing the LM that does not make it onto the target substrate. These techniques are also among the lowest resolution and have the worst line-edge roughness of the methods discussed in this review. Nevertheless, they produce exposed metallic features in which componentry can be added rapidly by pick-and-place tools.

Additive manufacturing techniques (e.g., direct ink writing) are known to be suited for rapid prototyping purposes rather than large scale manufacturing since each printhead can only build one piece at a time. That said, patterning techniques like shear-based direct writing of LM and extrusion-based 3D printing of LM pastes are attractive because they can be computer controlled (likewise for laser sintering of intricate designs on LM particle films). With few distinct steps, minimal manual intervention, and little material wastage (particularly for drop-on-demand printing modes), direct writing approaches have progressed the furthest in terms of commercial adoption and development (e.g., Feel the Same Inc. uses LM printing technology to produce soft sensors in wearable VR products; Xerox recently released the ElemX, a liquid metal printer that dispenses molten aluminum alloys; several start-up companies are exploring LMs for wearable devices).

Finally, techniques that use existing patterning tools—such as lithographic tools—seem to also be good candidates for manufacturing by harnessing established infrastructure. For example, selective wetting of LM to patterned metallic traces is straightforward.

5.9. Combining LM with New Materials

In many examples, LM is patterned on or in elastomers. There are opportunities and challenges to pattern LM in other materials,

such as hydrogels,[78,224,225] ionogels, biological/natural materials (e.g., tissue), and engineering materials (e.g., concrete). In aqueous environments, the oxide changes to GaOOH and is less passivating.[38] Can this issue be addressed to improve long term stability in aqueous applications?[226]

5.10. The Oxide

The native oxide that forms on LM is important for almost all the existing patterning techniques. It has been studied spectroscopically, its thickness is known to be a few nm, and its impact on rheology is well understood. Yet, the exact composition (as a function of depth) and physical properties (conductivity) are not fully understood.[227] There are opportunities to modify the oxide chemically and physically, as well as deposit materials on the surface that modify the properties.[31,228]

5.11. High Surface Area

There have been essentially no reports of methods to create high surface area LM structures. LM particles do not naturally form conductive, percolated networks until they are mechanically sintered, yet sintering causes particles to partially or completely merge, thereby decreasing the amount of exposed area. Such high surface area electrodes may find use for sensing and energy harvesting.

5.12. Reliability

The native oxide that forms on LM is important for most patterning methods. Yet, stretching a LM structure for the first time will break the oxide, causing exposed metal to oxidize. What happens when LM conductors are strain cycled many times? Does the oxide provide a barrier to oxidation or does the oxide thicken with use? Is this consequential for the performance? Strain cycling experiments reported in the literature suggest that LM conductors are reliable, but more studies are needed in demanding environments.

5.13. New Functions

LM patterning has been primarily used for creating electronic components such as interconnects, wires, antennas, and sensors, but there are other interesting applications. They have been used for batteries because of their ability to heal during cycling.[229] They can be used in reconfigurable optical devices.[230,231] Using interfacial modification of the oxide, LMs have been used for diodes and memristor devices.[232,233] Droplets of metal have been used for soft actuators[234] and switches[200] (transistor mimics). Soft circuits consisting of LM can change resistance when deformed and can be designed to perform "tactile logic" with semiconductors. Can additional components—such as soft capacitors and resistors—be combined to form more complex circuitry? LMs are also reactive and can be used to initiate polymerization or trigger redox reactions. Patterning LM could enable "active materials" that can respond to their environment or evolve materials as a function of time. Finally, could patterned LM be used for haptics?

Acknowledgements

J.M. and F.K. contributed equally to this work. The authors acknowledge support from the National Science Foundation ASSIST ERC (ASSIST, EEC-1160483), Indium Corporation, NSF Center for Dielectrics and Piezoelectrics (CDP, EEC-1841466), NSF (CMMI-2032415), and NCROEP. The authors appreciate the help of Val Gomez for creating an illustration for Figure 1. The title of this work was inspired by the authors' friend, the late Prof. Siegfried Bauer, who creatively used the term "soft future" to inspire the field.

Conflict of Interest

The authors declare no conflict of interest.

Keywords

composites, liquid metal, soft electronics, stretchable electronics, patterning

Received: June 8, 2022
Revised: August 23, 2022
Published online: March 9, 2023

[1] J. W. Strutt, L. Rayleigh, *Proc. London Math. Soc* **1878**, *10*, 4.
[2] G. D. Martin, S. D. Hoath, I. M. Hutchings, *J. Phys.: Conf. Ser.* **2008**, *105*, 012001.
[3] J. D. Paulsen, *Annu. Rev. Condens. Matter Phys.* **2019**, *10*, 431.
[4] D. Kumar, T. P. Russell, B. Davidovitch, N. Menon, *Nat. Mater.* **2020**, *19*, 690.
[5] J. D. Paulsen, V. Démery, C. D. Santangelo, T. P. Russell, B. Davidovitch, N. Menon, *Nat. Mater.* **2015**, *14*, 1206.
[6] M. D. Dickey, *ACS Appl. Mater. Interfaces* **2014**, *6*, 18369.
[7] J. Forth, X. Liu, J. Hasnain, A. Toor, K. Miszta, S. Shi, P. L. Geissler, T. Emrick, B. A. Helms, T. P. Russell, *Adv. Mater.* **2018**, *30*, 1707603.
[8] T. Daeneke, K. Khoshmanesh, N. Mahmood, I. A. De Castro, D. Esrafilzadeh, S. Barrow, M. Dickey, K. Kalantar-Zadeh, *Chem. Soc. Rev.* **2018**, *47*, 4073.
[9] S.-Y. Tang, C. Tabor, K. Kalantar-Zadeh, M. D. Dickey, *Annu. Rev. Mater. Res.* **2021**, *51*, 381.
[10] Q. Wang, Y. Yu, J. Liu, *Adv. Eng. Mater.* **2018**, *20*, 1700781.
[11] M. D. Dickey, *Phys. Today* **2021**, *74*, 30.
[12] D. Amoabeng, S. S. Velankar, *Polym. Eng. Sci.* **2018**, *58*, 1010.
[13] M. M. Markowitz, *J. Chem. Educ.* **1963**, *40*, 633.
[14] G. Stancari, L. Corradi, A. Dainelli, *Nucl. Instrum. Methods Phys. Res., Sect. A* **2008**, *594*, 321.
[15] R. A. Bernhoft, *J. Environ. Public Health* **2012**, *2012*, 460508.
[16] Y. Lu, Q. Hu, Y. Lin, D. B. Pacardo, C. Wang, W. Sun, F. S. Ligler, M. D. Dickey, Z. Gu, *Nat. Commun.* **2015**, *6*, 10066.
[17] L. J. Briggs, *J. Chem. Phys.* **1957**, *26*, 784.
[18] M. H. Malakooti, N. Kazem, J. Yan, C. Pan, E. J. Markvicka, K. Matyjaszewski, C. Majidi, *Adv. Funct. Mater.* **2019**, *29*, 1906098.
[19] Y. Zhang, J. R. Evans, S. Yang, *J. Chem. Eng. Data* **2011**, *56*, 328.
[20] A. R. Jacob, D. P. Parekh, M. D. Dickey, L. C. Hsiao, *Langmuir* **2019**, *35*, 11774.

[21] K. Spells, *Proc. Phys. Soc.* **1936**, *48*, 299.
[22] G. Abbaschian, *J. Less Common Metals* **1975**, *40*, 329.
[23] H. E. Sostman, *Rev. Sci. Instrum.* **1977**, *48*, 127.
[24] J. M. Chabala, *Phys. Rev. B* **1992**, *46*, 11346.
[25] Y. Ding, M. Zeng, L. Fu, *Matter* **2020**, *3*, 1477.
[26] A. Plech, U. Klemradt, H. Metzger, J. Peisl, *J. Phys.: Condens. Matter* **1998**, *10*, 971.
[27] T. Liu, P. Sen, C.-J. Kim, *J. Microelectromech. Syst.* **2011**, *21*, 443.
[28] N. Cabrera, N. F. Mott, *Rep. Prog. Phys.* **1949**, *12*, 163.
[29] Z. J. Farrell, C. Tabor, *Langmuir* **2018**, *34*, 234.
[30] L. Castilla-Amorós, T.-C. C. Chien, J. R. Pankhurst, R. Buonsanti, *J. Am. Chem. Soc.* **2022**, *144*, 1993.
[31] K. Y. Kwon, V. K. Truong, F. Krisnadi, S. Im, J. Ma, N. Mehrabian, T.-i. Kim, M. D. Dickey, *Adv. Intell. Syst.* **2021**, *3*, 2000159.
[32] N. Syed, A. Zavabeti, K. A. Messalea, E. Della Gaspera, A. Elbourne, A. Jannat, M. Mohiuddin, B. Y. Zhang, G. Zheng, L. Wang, *J. Am. Chem. Soc.* **2018**, *141*, 104.
[33] Y. Lin, C. Cooper, M. Wang, J. J. Adams, J. Genzer, M. D. Dickey, *Small* **2015**, *11*, 6397.
[34] M. Regan, H. Tostmann, P. S. Pershan, O. Magnussen, E. DiMasi, B. Ocko, M. Deutsch, *Phys. Rev. B* **1997**, *55*, 10786.
[35] S. Runde, H. Ahrens, F. Lawrenz, A. Sebastian, S. Block, C. A. Helm, *Adv. Mater. Interfaces* **2018**, *5*, 1800323.
[36] A. Zavabeti, J. Z. Ou, B. J. Carey, N. Syed, R. Orrell-Trigg, E. L. Mayes, C. Xu, O. Kavehei, A. P. O'Mullane, R. B. Kaner, *Science* **2017**, *358*, 332.
[37] A. Zavabeti, B. Y. Zhang, I. A. de Castro, J. Z. Ou, B. J. Carey, M. Mohiuddin, R. Datta, C. Xu, A. P. Mouritz, C. F. McConville, *Adv. Funct. Mater.* **2018**, *28*, 1804057.
[38] M. R. Khan, C. Trlica, J.-H. So, M. Valeri, M. D. Dickey, *ACS Appl. Mater. Interfaces* **2014**, *6*, 22467.
[39] R. C. Chiechi, E. A. Weiss, M. D. Dickey, G. M. Whitesides, *Angew. Chem., Int. Ed.* **2008**, *47*, 142.
[40] I. D. Joshipura, K. A. Persson, V. K. Truong, J.-H. Oh, M. Kong, M. H. Vong, C. Ni, M. Alsafatwi, D. P. Parekh, H. Zhao, M. D. Dickey, *Langmuir* **2021**, *37*, 10914.
[41] K. Doudrick, S. Liu, E. M. Mutunga, K. L. Klein, V. Damle, K. K. Varanasi, K. Rykaczewski, *Langmuir* **2014**, *30*, 6867.
[42] M. R. Khan, J. Bell, M. D. Dickey, *Adv. Mater. Interfaces* **2016**, *3*, 1600546.
[43] Y. Yoon, D. Kim, J.-B. Lee, *Micro Nano Syst. Lett.* **2014**, *2*, 3.
[44] R. K. Kramer, J. W. Boley, H. A. Stone, J. C. Weaver, R. J. Wood, *Langmuir* **2014**, *30*, 533.
[45] I. D. Joshipura, H. R. Ayers, G. A. Castillo, C. Ladd, C. E. Tabor, J. J. Adams, M. D. Dickey, *ACS Appl. Mater. Interfaces* **2018**, *10*, 44686.
[46] M. D. Dickey, R. C. Chiechi, R. J. Larsen, E. A. Weiss, D. A. Weitz, G. M. Whitesides, *Adv. Funct. Mater.* **2008**, *18*, 1097.
[47] R. J. Larsen, M. D. Dickey, G. M. Whitesides, D. A. Weitz, *J. Rheol.* **2009**, *53*, 1305.
[48] A. Tabatabai, A. Fassler, C. Usiak, C. Majidi, *Langmuir* **2013**, *29*, 6194.
[49] A. Cook, D. P. Parekh, C. Ladd, G. Kotwal, L. Panich, M. Durstock, M. D. Dickey, C. E. Tabor, *Adv. Eng. Mater.* **2019**, *21*, 1900400.
[50] C. Ladd, J.-H. So, J. Muth, M. D. Dickey, *Adv. Mater.* **2013**, *25*, 5081.
[51] S. Liu, S. N. Reed, M. J. Higgins, M. S. Titus, R. Kramer-Bottiglio, *Nanoscale* **2019**, *11*, 17615.
[52] M. D. Bartlett, A. Fassler, N. Kazem, E. J. Markvicka, P. Mandal, C. Majidi, *Adv. Mater.* **2016**, *28*, 3726.
[53] E. J. Markvicka, M. D. Bartlett, X. Huang, C. Majidi, *Nat. Mater.* **2018**, *17*, 618.
[54] R. Tutika, A. B. M. T. Haque, M. D. Bartlett, *Commun. Mater.* **2021**, *2*, 64.
[55] M. D. Bartlett, N. Kazem, M. J. Powell-Palm, X. Huang, W. Sun, J. A. Malen, C. Majidi, *Proc. Natl. Acad. Sci. USA* **2017**, *114*, 2143.
[56] S. Chen, H.-Z. Wang, R.-Q. Zhao, W. Rao, J. Liu, *Matter* **2020**, *2*, 1446.
[57] R. W. Style, R. Tutika, J. Y. Kim, M. D. Bartlett, *Adv. Funct. Mater.* **2021**, *31*, 2005804.
[58] D. R. Lide, *CRC Handbook of Chemistry and Physics*, Vol. *85*, CRC Press, Boca Raton, FL **2004**.
[59] D. Zrnic, D. Swatik, *J. Less Common Metals* **1969**, *18*, 67.
[60] J. Ma, V. T. Bharambe, K. A. Persson, A. L. Bachmann, I. D. Joshipura, J. Kim, K. H. Oh, J. F. Patrick, J. J. Adams, M. D. Dickey, *ACS Appl. Mater. Interfaces* **2021**, *13*, 12709.
[61] M. L. Ramires, C. A. Nieto de Castro, Y. Nagasaka, A. Nagashima, M. J. Assael, W. A. Wakeham, *J. Phys. Chem. Ref. Data* **1995**, *24*, 1377.
[62] L. Sanchez-Botero, D. S. Shah, R. Kramer-Bottiglio, *Adv. Mater.* **2022**, *34*, 2109427.
[63] N. Zolfaghari, P. Khandagale, M. J. Ford, K. Dayal, C. Majidi, *Soft Matter* **2020**, *16*, 8818.
[64] I. D. Joshipura, H. R. Ayers, C. Majidi, M. D. Dickey, *J. Mater. Chem. C* **2015**, *3*, 3834.
[65] M. Khondoker, D. Sameoto, *Smart Mater. Struct.* **2016**, *25*, 093001.
[66] S. Zhu, J.-H. So, R. Mays, S. Desai, W. R. Barnes, B. Pourdeyhimi, M. D. Dickey, *Adv. Funct. Mater.* **2013**, *23*, 2308.
[67] G. Mao, M. Drack, M. Karami-Mosammam, D. Wirthl, T. Stockinger, R. Schwödiauer, M. Kaltenbrunner, *Sci. Adv.* **2020**, *6*, eabc0251.
[68] Y. Lin, O. Gordon, M. R. Khan, N. Vasquez, J. Genzer, M. D. Dickey, *Lab Chip* **2017**, *17*, 3043.
[69] V. Bharambe, D. P. Parekh, C. Ladd, K. Moussa, M. D. Dickey, J. J. Adams, *Addit. Manuf.* **2017**, *18*, 221.
[70] H.-J. Kim, T. Maleki, P. Wei, B. Ziaie, *J. Microelectromech. Syst.* **2009**, *18*, 138.
[71] D. Lide, CRC Handbook of Chemistry and Physics, Taylor & Francis, Boca Raton, FL, USA **2007**.
[72] Y. Qu, T. Nguyen-Dang, A. G. Page, W. Yan, T. Das Gupta, G. M. Rotaru, R. M. Rossi, V. D. Favrod, N. Bartolomei, F. Sorin, *Adv. Mater.* **2018**, *30*, 1707251.
[73] C. Dong, A. Leber, T. Das Gupta, R. Chandran, M. Volpi, Y. Qu, T. Nguyen-Dang, N. Bartolomei, W. Yan, F. Sorin, *Nat. Commun.* **2020**, *11*, 3537.
[74] Z. Ma, Q. Huang, Q. Xu, Q. Zhuang, X. Zhao, Y. Yang, H. Qiu, Z. Yang, C. Wang, Y. Chai, *Nat. Mater.* **2021**, *20*, 859.
[75] J. E. Park, H. S. Kang, M. Koo, C. Park, *Adv. Mater.* **2020**, *32*, 2002178.
[76] N. Kazem, M. D. Bartlett, C. Majidi, *Adv. Mater.* **2018**, *30*, 1706594.
[77] M. D. Bartlett, R. W. Style, *Soft Matter* **2020**, *16*, 5799.
[78] Y. Y. Choi, D. H. Ho, J. H. Cho, *ACS Appl. Mater. Interfaces* **2020**, *12*, 9824.
[79] D. Kim, Y. Yoon, S. K. Kauh, J. Lee, *Adv. Funct. Mater.* **2018**, *28*, 1800380.
[80] J. Monahan, A. A. Gewirth, R. G. Nuzzo, *Anal. Chem.* **2001**, *73*, 3193.
[81] L. Teng, S. Ye, S. Handschuh-Wang, X. Zhou, T. Gan, X. Zhou, *Adv. Funct. Mater.* **2019**, *29*, 1808739.
[82] J. B. Andrews, K. Mondal, T. V. Neumann, J. A. Cardenas, J. Wang, D. P. Parekh, Y. Lin, P. Ballentine, M. D. Dickey, A. D. Franklin, *ACS Nano* **2018**, *12*, 5482.
[83] K. S. Reichel, N. Lozada-Smith, I. D. Joshipura, J. Ma, R. Shrestha, R. Mendis, M. D. Dickey, D. M. Mittleman, *Nat. Commun.* **2018**, *9*, 4202.
[84] N. Ilyas, A. Cook, C. E. Tabor, *Adv. Mater. Interfaces* **2017**, *4*, 1700141.
[85] Y.-G. Park, H. S. An, J.-Y. Kim, J.-U. Park, *Sci. Adv.* **2019**, *5*, eaaw2844.
[86] Y. Yoon, S. Kim, D. Kim, S. K. Kauh, J. Lee, *Adv. Mater. Technol.* **2019**, *4*, 1800379.

[87] B. Ma, C. Xu, J. Chi, J. Chen, C. Zhao, H. Liu, *Adv. Funct. Mater.* **2019**, *29*, 1901370.
[88] D. P. Parekh, C. Ladd, L. Panich, K. Moussa, M. D. Dickey, *Lab Chip* **2016**, *16*, 1812.
[89] S. Kim, J. Oh, D. Jeong, W. Park, J. Bae, *Soft Rob.* **2018**, *5*, 601.
[90] S. Kim, J. Oh, D. Jeong, J. Bae, *ACS Appl. Mater. Interfaces* **2019**, *11*, 20557.
[91] Y. Gao, H. Li, J. Liu, *PLoS One* **2012**, *7*, e45485.
[92] J. W. Boley, E. L. White, G. T. C. Chiu, R. K. Kramer, *Adv. Funct. Mater.* **2014**, *24*, 3501.
[93] A. M. Watson, A. B. Cook, C. E. Tabor, *Adv. Eng. Mater.* **2019**, *21*, 1900397.
[94] A. Gannarapu, B. A. Gozen, *Adv. Mater. Technol.* **2016**, *1*, 1600047.
[95] Y. Zheng, Z.-Z. He, J. Yang, J. Liu, *Sci. Rep.* **2015**, *4*, 4588.
[96] T. V. Neumann, M. D. Dickey, *Adv. Mater. Technol.* **2020**, *5*, 2000070.
[97] D. Foresti, K. T. Kroll, R. Amissah, F. Sillani, K. A. Homan, D. Poulikakos, J. A. Lewis, *Sci. Adv.* **2018**, *4*, eaat1659.
[98] N. Lazarus, S. S. Bedair, I. M. Kierzewski, *ACS Appl. Mater. Interfaces* **2017**, *9*, 1178.
[99] T. Neumann, B. Kara, Y. Sargolzaeiaval, S. Im, J. Ma, J. Yang, M. Ozturk, M. Dickey, *Micromachines* **2021**, *12*, 146.
[100] T. H. Park, J. H. Kim, S. Seo, *Adv. Funct. Mater.* **2020**, *30*, 2003694.
[101] L. Wang, J. Liu, *RSC Adv.* **2015**, *5*, 57686.
[102] J. Liu, S. Yang, Z. Liu, H. Guo, Z. Liu, Z. Xu, C. Liu, L. Wang, *J. Micromech. Microeng.* **2019**, *29*, 095001.
[103] A. F. Silva, H. Paisana, T. Fernandes, J. Góis, A. Serra, J. F. J. Coelho, A. T. Almeida, C. Majidi, M. Tavakoli, *Adv. Mater. Technol.* **2020**, *5*, 2000343.
[104] K. S. Elassy, T. K. Akau, W. A. Shiroma, S. Seo, A. T. Ohta, *Appl. Sci.* **2019**, *9*, 1565.
[105] C. W. Park, Y. G. Moon, H. Seong, S. W. Jung, J.-Y. Oh, B. S. Na, N.-M. Park, S. S. Lee, S. G. Im, J. B. Koo, *ACS Appl. Mater. Interfaces* **2016**, *8*, 15459.
[106] C. Guo, Y. Yu, J. Liu, *J. Mater. Chem. B* **2014**, *2*, 5739.
[107] H. Gui, S. Tan, Q. Wang, Y. Yu, F. Liu, J. Lin, J. Liu, *Sci. China Technol. Sci.* **2017**, *60*, 306.
[108] J. Melcher, K. Elassy, R. Ordonez, C. Hayashi, A. Ohta, D. Garmire, *Micromachines* **2019**, *10*, 54.
[109] M. Wang, C. Ma, P. C. Uzabakiriho, X. Chen, Z. Chen, Y. Cheng, Z. Wang, G. Zhao, *ACS Nano* **2021**, *15*, 19364.
[110] Q. Zhang, Y. Gao, J. Liu, *Appl. Phys. A* **2014**, *116*, 1091.
[111] S. H. Jeong, K. Hjort, Z. Wu, *Sci. Rep.* **2015**, *5*, 8419.
[112] M. R. Khan, C. Trlica, M. D. Dickey, *Adv. Funct. Mater.* **2015**, *25*, 671.
[113] Y.-C. Sun, G. Boero, J. r. Brugger, *ACS Appl. Electron. Mater.* **2021**, *3*, 5423.
[114] R. Guo, J. Tang, S. Dong, J. Lin, H. Wang, J. Liu, W. Rao, *Adv. Mater. Technol.* **2018**, *3*, 1800265.
[115] Q. Wang, Y. Yu, J. Yang, J. Liu, *Adv. Mater.* **2015**, *27*, 7109.
[116] R. Guo, X. Sun, B. Yuan, H. Wang, J. Liu, *Adv. Sci.* **2019**, *6*, 1901478.
[117] M. g. Kim, C. Kim, H. Alrowais, O. Brand, *Adv. Mater. Technol.* **2018**, *3*, 1800061.
[118] Y. Mao, Y. Wu, P. Zhang, Y. Yu, Z. He, Q. Wang, *J. Mater. Sci. Technol.* **2021**, *61*, 132.
[119] M.-g. Kim, D. K. Brown, O. Brand, *Nat. Commun.* **2020**, *11*, 1002.
[120] S. Jeong, K. Hjort, Z. Wu, *Sensors* **2014**, *14*, 16311.
[121] J. Jiang, W. Fei, M. Pu, Z. Chai, Z. Wu, *Adv. Mater. Interfaces* **2022**, *9*, 2200516.
[122] Y. Jiang, S. Su, H. Peng, H. Sing Kwok, X. Zhou, S. Chen, *J. Mater. Chem. C* **2017**, *5*, 12378.
[123] D. Kim, D. Jung, J. H. Yoo, Y. Lee, W. Choi, G. S. Lee, K. Yoo, J.-B. Lee, *J. Micromech. Microeng.* **2014**, *24*, 055018.
[124] S. S. Kadlaskar, J. H. Yoo, J. B. Lee, W. Choi, *J. Colloid Interface Sci.* **2017**, *492*, 33.
[125] Z. Chen, J. B. Lee, *ACS Appl. Mater. Interfaces* **2019**, *11*, 35488.
[126] K. L. Wilke, Z. Lu, Y. Song, E. N. Wang, *Proc. Natl. Acad. Sci. USA* **2022**, *119*, e2109052119 .
[127] K. Y. Kwon, S. Cheeseman, A. Frias-De-Diego, H. Hong, J. Yang, W. Jung, H. Yin, B. J. Murdoch, F. Scholle, N. Crook, *Adv. Mater.* **2021**, *33*, 2104298.
[128] A. Fassler, C. Majidi, *Lab Chip* **2013**, *13*, 4442.
[129] U. Daalkhaijav, O. D. Yirmibesoglu, S. Walker, Y. Mengüç, *Adv. Mater. Technol.* **2018**, *3*, 1700351.
[130] D. P. Parekh, C. M. Fancher, M. G. Mohammed, T. V. Neumann, D. Saini, J. Guerrier, C. Ladd, E. Hubbard, J. L. Jones, M. D. Dickey, *ACS Appl. Nano Mater.* **2020**, *3*, 12064.
[131] Y.-G. Park, H. Min, H. Kim, A. Zhexembekova, C. Y. Lee, J.-U. Park, *Nano Lett.* **2019**, *19*, 4866.
[132] H. Chang, P. Zhang, R. Guo, Y. Cui, Y. Hou, Z. Sun, W. Rao, *ACS Appl. Mater. Interfaces* **2020**, *12*, 14125.
[133] W. Kong, N. U. H. Shah, T. V. Neumann, M. H. Vong, P. Kotagama, M. D. Dickey, R. Y. Wang, K. Rykaczewski, *Soft Matter* **2020**, *16*, 5801.
[134] T. V. Neumann, E. G. Facchine, B. Leonardo, S. Khan, M. D. Dickey, *Soft Matter* **2020**, *16*, 6608.
[135] C. Wang, Y. Gong, B. V. Cunning, S. Lee, Q. Le, S. R. Joshi, O. Buyukcakir, H. Zhang, W. K. Seong, M. Huang, M. Wang, J. Lee, G.-H. Kim, R. S. Ruoff, *Sci. Adv.* **2021**, *7*, eabe3767.
[136] L. Cao, D. Yu, Z. Xia, H. Wan, C. Liu, T. Yin, Z. He, *Adv. Mater.* **2020**, *32*, 2000827.
[137] Y. Lin, J. Genzer, M. D. Dickey, *Adv. Sci.* **2020**, *7*, 2000192.
[138] A. Haake, R. Tutika, G. M. Schloer, M. D. Bartlett, E. J. Markvicka, *Adv. Mater.* **2022**, *34*, 2200182.
[139] A. Koh, J. Sietins, G. Slipher, R. Mrozek, *J. Mater. Res.* **2018**, *33*, 2443.
[140] M. G. Mohammed, R. Kramer, *Adv. Mater.* **2017**, *29*, 1604965.
[141] R. Tutika, S. Kmiec, A. T. Haque, S. W. Martin, M. D. Bartlett, *ACS Appl. Mater. Interfaces* **2019**, *11*, 17873.
[142] C. Pan, E. J. Markvicka, M. H. Malakooti, J. Yan, L. Hu, K. Matyjaszewski, C. Majidi, *Adv. Mater.* **2019**, *31*, 1900663.
[143] J. Yang, D. Tang, J. Ao, T. Ghosh, T. V. Neumann, D. Zhang, E. Piskarev, T. Yu, V. K. Truong, K. Xie, *Adv. Funct. Mater.* **2020**, *30*, 2002611.
[144] K. Parida, G. Thangavel, G. Cai, X. Zhou, S. Park, J. Xiong, P. S. Lee, *Nat. Commun.* **2019**, *10*, 2158.
[145] J. Wang, G. Cai, S. Li, D. Gao, J. Xiong, P. S. Lee, *Adv. Mater.* **2018**, *30*, 1706157.
[146] J. Wang, S. Liu, S. Guruswamy, A. Nahata, *Adv. Opt. Mater.* **2014**, *2*, 663.
[147] M. A. Khondoker, A. Ostashek, D. Sameoto, *Adv. Eng. Mater.* **2019**, *21*, 1900060.
[148] J. Zhang, Q. Lu, Y. Li, T. Li, M.-H. Lu, Y.-F. Chen, D. Kong, *ACS Mater. Lett.* **2021**, *3*, 1104.
[149] S. Liu, M. C. Yuen, E. L. White, J. W. Boley, B. Deng, G. J. Cheng, R. Kramer-Bottiglio, *ACS Appl. Mater. Interfaces* **2018**, *10*, 28232.
[150] A. S. Utada, A. Fernandez-Nieves, H. A. Stone, D. A. Weitz, *Phys. Rev. Lett.* **2007**, *99*, 094502.
[151] M. Song, K. Kartawira, K. D. Hillaire, C. Li, C. B. Eaker, A. Kiani, K. E. Daniels, M. D. Dickey, *Proc. Natl. Acad. Sci. USA* **2020**, *117*, 19026.
[152] Y. He, J. Tang, K. Kalantar-Zadeh, M. D. Dickey, X. Wang, *Proc. Natl. Acad. Sci. USA* **2022**, *119*, e2117535119.
[153] Y. Lin, C. Ladd, S. Wang, A. Martin, J. Genzer, S. A. Khan, M. D. Dickey, *Extreme Mech. Lett.* **2016**, *7*, 55.
[154] C. B. Cooper, K. Arutselvan, Y. Liu, D. Armstrong, Y. Lin, M. R. Khan, J. Genzer, M. D. Dickey, *Adv. Funct. Mater.* **2017**, *27*, 1605630.
[155] R. Lin, H.-J. Kim, S. Achavananthadith, Z. Xiong, J. K. Lee, Y. L. Kong, J. S. Ho, *Nat. Commun.* **2022**, *13*, 1.

[156] Y. C. Lai, H. W. Lu, H. M. Wu, D. Zhang, J. Yang, J. Ma, M. Shamsi, V. Vallem, M. D. Dickey, *Adv. Energy Mater.* **2021**, *11*, 2100411.
[157] A. Hirsch, S. P. Lacour, *Adv. Sci.* **2018**, *5*, 1800256.
[158] H. Zhu, S. Wang, M. Zhang, T. Li, G. Hu, D. Kong, *npj Flexible Electron.* **2021**, *5*, 25.
[159] G. Li, X. Wu, D.-W. Lee, *Sens. Actuators, B* **2015**, *221*, 1114.
[160] J. Norkett, M. Dickey, V. Miller, *Metall. Mater. Trans. A* **2021**, *52*, 2158.
[161] C. Xiao, J. Feng, H. Xu, R. Xu, T. Zhou, *ACS Appl. Mater. Interfaces* **2022**, *14*, 20000.
[162] B. A. Gozen, A. Tabatabai, O. B. Ozdoganlar, C. Majidi, *Adv. Mater.* **2014**, *26*, 5211.
[163] Y. Liu, X. Ji, J. Liang, *npj Flexible Electron.* **2021**, *5*, 11.
[164] J. W. Boley, E. L. White, R. K. Kramer, *Adv. Mater.* **2015**, *27*, 2355.
[165] C. J. Thrasher, Z. J. Farrell, N. J. Morris, C. L. Willey, C. E. Tabor, *Adv. Mater.* **2019**, *31*, 1903864.
[166] L. Tang, S. Cheng, L. Zhang, H. Mi, L. Mou, S. Yang, Z. Huang, X. Shi, X. Jiang, *iScience* **2018**, *4*, 302.
[167] S. Liu, M. C. Yuen, R. Kramer-Bottiglio, *Flexible Printed Electron.* **2019**, *4*, 015004.
[168] M. C. Yuen, M. A. Creighton, C. E. Tabor, in *2020 3rd IEEE Int. Conf. on Soft Robotics (RoboSoft)*, IEEE, Piscataway, NJ, USA, May-July **2020**, pp. 676–681.
[169] L. y. Zhou, J. z. Fu, Q. Gao, P. Zhao, Y. He, *Adv. Funct. Mater.* **2020**, *30*, 1906683.
[170] H. Wang, Y. Yao, Z. He, W. Rao, L. Hu, S. Chen, J. Lin, J. Gao, P. Zhang, X. Sun, *Adv. Mater.* **2019**, *31*, 1901337.
[171] S. Veerapandian, W. Jang, J. B. Seol, H. Wang, M. Kong, K. Thiyagarajan, J. Kwak, G. Park, G. Lee, W. Suh, *Nat. Mater.* **2021**, *20*, 533.
[172] W. Zhao, J. L. Bischof, J. Hutasoit, X. Liu, T. C. Fitzgibbons, J. R. Hayes, P. J. Sazio, C. Liu, J. K. Jain, J. V. Badding, *Nano Lett.* **2015**, *15*, 153.
[173] S. Park, K. Mondal, R. M. Treadway III, V. Kumar, S. Ma, J. D. Holbery, M. D. Dickey, *ACS Appl. Mater. Interfaces* **2018**, *10*, 11261.
[174] H. Li, R. Qiao, T. P. Davis, S.-Y. Tang, *Biosensors* **2020**, *10*, 196.
[175] Y. Ren, X. Sun, J. Liu, *Micromachines* **2020**, *11*, 200.
[176] K. Khoshmanesh, S.-Y. Tang, J. Y. Zhu, S. Schaefer, A. Mitchell, K. Kalantar-Zadeh, M. D. Dickey, *Lab Chip* **2017**, *17*, 974.
[177] P. Sen, C.-J. C. Kim, *IEEE Trans. Ind. Electron.* **2008**, *56*, 1314.
[178] K. N. Paracha, A. D. Butt, A. S. Alghamdi, S. A. Babale, P. J. Soh, *Sensors* **2020**, *20*, 177.
[179] T. Kim, D.-m. Kim, B. J. Lee, J. Lee, *Sensors* **2019**, *19*, 4250.
[180] M. Zadan, C. Chiew, C. Majidi, M. H. Malakooti, *Multifunct. Mater.* **2021**, *4*, 012001.
[181] V. Vallem, Y. Sargolzaeiaval, M. Ozturk, Y. C. Lai, M. D. Dickey, *Adv. Mater.* **2021**, *33*, 2004832.
[182] J. Park, S. Wang, M. Li, C. Ahn, J. K. Hyun, D. S. Kim, D. K. Kim, J. A. Rogers, Y. Huang, S. Jeon, *Nat. Commun.* **2012**, *3*, 916.
[183] A. Hirsch, H. O. Michaud, A. P. Gerratt, S. de Mulatier, S. P. Lacour, *Adv. Mater.* **2016**, *28*, 4507.
[184] M. D. Dickey, *Adv. Mater.* **2017**, *29*, 1606425.
[185] J. Oh, S. Kim, S. Lee, S. Jeong, S. H. Ko, J. Bae, *Adv. Funct. Mater.* **2021**, *31*, 2007772.
[186] Y. Zhang, S. Liu, Y. Miao, H. Yang, X. Chen, X. Xiao, Z. Jiang, X. Chen, B. Nie, J. Liu, *ACS Appl. Mater. Interfaces* **2020**, *12*, 27961.
[187] G. Li, D.-W. Lee, *Lab Chip* **2017**, *17*, 3415.
[188] J. Chen, J. Zhang, Z. Luo, J. Zhang, L. Li, Y. Su, X. Gao, Y. Li, W. Tang, C. Cao, Q. Liu, L. Wang, H. Li, *ACS Appl. Mater. Interfaces* **2020**, *12*, 22200.
[189] N. Lazarus, C. Meyer, S. Bedair, H. Nochetto, I. Kierzewski, *Smart Mater. Struct.* **2014**, *23*, 085036.
[190] X. Zhang, J. Ai, Z. Ma, Y. Yin, R. Zou, B. Su, *Adv. Funct. Mater.* **2020**, *30*, 2003680.
[191] T. Hu, S. Xuan, L. Ding, X. Gong, *Sens. Actuators, B* **2020**, *314*, 128095.
[192] Q. Gao, H. Li, J. Zhang, Z. Xie, J. Zhang, L. Wang, *Sci. Rep.* **2019**, *9*, 5908.
[193] L. Zhang, M. Gao, R. Wang, Z. Deng, L. Gui, *Sensors* **2019**, *19*, 1316.
[194] Y. Chen, Y. Liu, J. Ren, W. Yang, E. Shang, K. Ma, L. Zhang, J. Jiang, X. Sun, *Mater. Des.* **2020**, *190*, 108567.
[195] C. Votzke, U. Daalkhaijav, Y. Mengüç, M. L. Johnston, *IEEE Sens. J.* **2019**, *19*, 3832.
[196] K. B. Ozutemiz, J. Wissman, O. B. Ozdoganlar, C. Majidi, *Adv. Mater. Interfaces* **2018**, *5*, 1701596.
[197] F. Krisnadi, L. L. Nguyen, J. Ma, M. R. Kulkarni, N. Mathews, M. D. Dickey, *Adv. Mater.* **2020**, *32*, 2001642.
[198] D. Kim, J. H. Yoo, W. Choi, K. Yoo, J.-B. J. Lee, in *2014 IEEE 27th Int. Conf. on Micro Electro Mechanical Systems (MEMS)*, IEEE, Piscataway, NJ, USA, January **2014**, pp. 540–543.
[199] M. R. Khan, C. B. Eaker, E. F. Bowden, M. D. Dickey, *Proc. Natl. Acad. Sci. USA* **2014**, *111*, 14047.
[200] J. Wissman, M. D. Dickey, C. Majidi, *Adv. Sci.* **2017**, *4*, 1700169.
[201] M. Song, K. E. Daniels, A. Kiani, S. Rashid-Nadimi, M. D. Dickey, *Adv. Intell. Syst.* **2021**, *3*, 2100024.
[202] Y. Yang, N. Sun, Z. Wen, P. Cheng, H. Zheng, H. Shao, Y. Xia, C. Chen, H. Lan, X. Xie, *ACS Nano* **2018**, *12*, 2027.
[203] Y. Huang, Y. Ding, J. Bian, Y. Su, J. Zhou, Y. Duan, Z. Yin, *Nano Energy* **2017**, *40*, 432.
[204] V. Vallem, E. Roosa, T. Ledinh, W. Jung, T. i. Kim, S. Rashid-Nadimi, A. Kiani, M. D. Dickey, *Adv. Mater.* **2021**, *33*, 2103142.
[205] M. Zadan, M. H. Malakooti, C. Majidi, *ACS Appl. Mater. Interfaces* **2020**, *12*, 17921.
[206] H. Zou, Y. Zhang, L. Guo, P. Wang, X. He, G. Dai, H. Zheng, C. Chen, A. C. Wang, C. Xu, *Nat. Commun.* **2019**, *10*, 1.
[207] D. J. Lacks, T. Shinbrot, *Nat. Rev. Chem.* **2019**, *3*, 465.
[208] S. Gao, R. Wang, C. Ma, Z. Chen, Y. Wang, M. Wu, Z. Tang, N. Bao, D. Ding, W. Wu, *J. Mater. Chem. A* **2019**, *7*, 7109.
[209] C. Pan, D. Liu, M. J. Ford, C. Majidi, *Adv. Mater. Technol.* **2020**, *5*, 2000754.
[210] C. Yang, J. He, Y. Guo, D. Zhao, X. Hou, J. Zhong, S. Zhang, M. Cui, X. Chou, *Mater. Des.* **2021**, *201*, 109508.
[211] S. Bauer, S. Bauer-Gogonea, I. Graz, M. Kaltenbrunner, C. Keplinger, R. Schwödiauer, *Adv. Mater.* **2014**, *26*, 149.
[212] J. K. Moon, J. Jeong, D. Lee, H. K. Pak, *Nat. Commun.* **2013**, *4*, 1487.
[213] N. Jaziri, A. Boughamoura, J. Müller, B. Mezghani, F. Tounsi, M. Ismail, *Energy Rep.* **2020**, *6*, 264.
[214] A. Nozariasbmarz, H. Collins, K. Dsouza, M. H. Polash, M. Hosseini, M. Hyland, J. Liu, A. Malhotra, F. M. Ortiz, F. Mohaddes, *Appl. Energy* **2020**, *258*, 114069.
[215] S. H. Jeong, F. J. Cruz, S. Chen, L. Gravier, J. Liu, Z. Wu, K. Hjort, S.-L. Zhang, Z.-B. Zhang, *ACS Appl. Mater. Interfaces* **2017**, *9*, 15791.
[216] F. Suarez, D. P. Parekh, C. Ladd, D. Vashaee, M. D. Dickey, M. C. Öztürk, *Appl. Energy* **2017**, *202*, 736.
[217] Y. Sargolzaeiaval, V. P. Ramesh, T. V. Neumann, V. Misra, D. Vashaee, M. D. Dickey, M. C. Öztürk, *Appl. Energy* **2020**, *262*, 114370.
[218] C. Pan, K. Kumar, J. Li, E. J. Markvicka, P. R. Herman, C. Majidi, *Adv. Mater.* **2018**, *30*, 1706937.
[219] I. S. Maksymov, A. D. Greentree, *Phys. Rev. A* **2017**, *96*, 043829.
[220] P. Reineck, Y. Lin, B. C. Gibson, M. D. Dickey, A. D. Greentree, I. S. Maksymov, *Sci. Rep.* **2019**, *9*, 5345.
[221] M. A. Creighton, M. C. Yuen, N. J. Morris, C. E. Tabor, *Nanoscale* **2020**, *12*, 23995.
[222] E. B. Secor, A. B. Cook, C. E. Tabor, M. C. Hersam, *Adv. Electron. Mater.* **2018**, *4*, 1700483.
[223] T. Lu, E. J. Markvicka, Y. Jin, C. Majidi, *ACS Appl. Mater. Interfaces* **2017**, *9*, 22055.

[224] T. Shay, O. D. Velev, M. D. Dickey, *Soft Matter* **2018**, *14*, 3296.
[225] J.-E. Park, H. S. Kang, J. Baek, T. H. Park, S. Oh, H. Lee, M. Koo, C. Park, *ACS Nano* **2019**, *13*, 9122.
[226] X. Huang, T. Xu, A. Shen, T. P. Davis, R. Qiao, S.-Y. Tang, *ACS Appl. Nano Mater.* **2022**, *5*, 5959.
[227] L. Cademartiri, M. M. Thuo, C. A. Nijhuis, W. F. Reus, S. Tricard, J. R. Barber, R. N. Sodhi, P. Brodersen, C. Kim, R. C. Chiechi, *J. Phys. Chem. C* **2012**, *116*, 10848.
[228] N. J. Morris, Z. J. Farrell, C. E. Tabor, *Nanoscale* **2019**, *11*, 17308.
[229] X. Guo, Y. Ding, G. Yu, *Adv. Mater.* **2021**, *33*, 2100052.
[230] K. Nakakubo, H. Yoshioka, K. Morita, R. Ishimatsu, A. Kiani, H. Hallen, M. D. Dickey, Y. Oki, *Opt. Mater. Express* **2021**, *11*, 2099.
[231] M. G. Mohammed, M. D. Dickey, *Sens. Actuators, A* **2013**, *193*, 246.
[232] J. H. So, H. J. Koo, M. D. Dickey, O. D. Velev, *Adv. Funct. Mater.* **2012**, *22*, 625.
[233] H. J. Koo, J. H. So, M. D. Dickey, O. D. Velev, *Adv. Mater.* **2011**, *23*, 3559.
[234] T. Cole, S.-Y. Tang, *Mater. Adv.* **2022**, *3*, 173.

Jinwoo Ma received a B.S. in materials science and engvineering from Seoul National University (2012) and a Ph.D. in materials science and engineering from Seoul National University (2020), under the guidance of Professor Kyu Hwan Oh and Jeong-Yun Sun. He worked in the Dickey group at NC State University as a visiting scholar, and subsequently as a postdoctoral researcher. Currently, he works at Samsung Electronics. His research interests include patterning and actuating liquid metals for flexible and stretchable electronics and actuating soft materials by harnessing smart polymer and interfacial bonding.

Febby Krisnadi received a B.Eng. in materials engineering from Nanyang Technological University (2020) under the guidance of Professor Nripan Mathews. She is currently a Ph.D. student advised by Professor Michael Dickey at NC State University. Her research interests include multiphasic composites, functional pastes, and electromechanical properties of soft materials.

Man Hou Vong received a B.S. in chemical engineering from Georgia Institute of Technology (2018). He is currently pursuing a Ph.D. in chemical engineering at NC State University under the guidance of Professor Michael Dickey. His current research interests include liquid metals and their composites, interfacial and wetting phenomena, and ultrathin metal oxides.

Minsik Kong received a B.S. in materials science and engineering from Pohang University of Science and Technology (POSTECH) in 2016. He is pursuing a Ph.D. degree under the supervision of Prof. Unyong Jeong in the same department. His research interests include interfacing issues in soft electronic devices and the characterization of surface oxides in liquid metals.

Omar M. Awartani received a B.S. in aerospace engineering from NC State University. In 2010, he joined Prof. Brendan O'Connor's group at NC State University, where he completed his M.S. and Ph.D. in mechanical engineering. From 2015–2017, he was a postdoctoral fellow in Prof. Harald Ade's group. Later he joined the American University of Beirut as an assistant professor in mechanical engineering and was a visiting professor at Prof. Michael Dickey's lab from 2020–2022. Currently he is a research scientist at Meta Reality Labs-Research. His research interests include soft and stretchable electronics, patterning of liquid metals, and formulating conductive inks.

Michael D. Dickey received a B.S. in chemical engineering from Georgia Institute of Technology (1999) and a Ph.D. from the University of Texas (2006) under the guidance of Professor Grant Willson. From 2006–2008 he was a post-doctoral fellow in the lab of Professor George Whitesides at Harvard University. He is currently the Camille and Henry Dreyfus Professor in the Department of Chemical and Biomolecular Engineering at NC State University. He completed a sabbatical at Microsoft in 2016. His research interests include soft matter (liquid metals, gels, polymers) for soft and stretchable devices (electronics, energy harvesters, textiles, and soft robotics).